Catalizzatori e combustione catalitica

Luciana Lisi – Giovanna Ruoppolo

Catalytic combustor:

Catalyst bed through which a pre-mixed and pre-heated fuel/air mixture is passed

It is able to carry out a complete combustion at low fuel concentration (low T) avoiding formation of *thermal NOx*

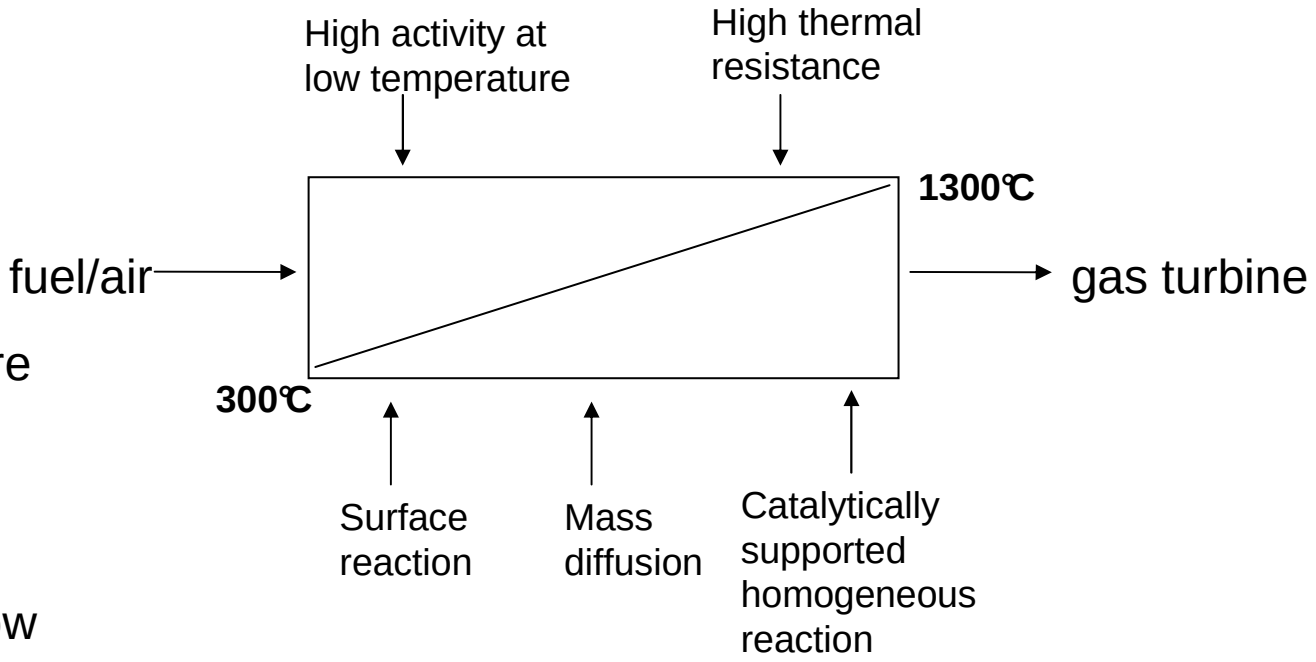

Region A: low temperature
kinetic regime
exponential increase of reaction rate
Region B: mass transfer control
low dependence on T
Region C: increase of T due to the exothermal reaction
homogeneous + heterogeneous reaction

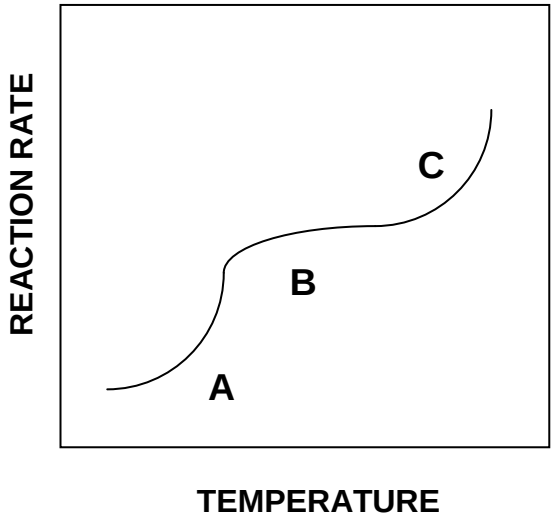

Catalytic system:

Active material

Support (substrate + washcoat)

Properties required to the catalytic system:

- **Ignition of the fuel/air mixture at T as low as possible (low light off temperature)**
- **Activity high enough to maintain complete combustion also at low air preheat or high mass throughput**
- **Large geometric surface area**
- **Low pressure drop**
- **Good thermal shock resistance**
- **High working temperature**
- **High surface area of the support also at high temperature**
- **Long life-time**

Support (substrate + washcoat)

Increases the surface area of the active component dispersed as small particles

Limits sintering of the active component and increase its thermal stability

Can improve activity through a positive interaction with the active component

Substrate

Ceramic substrates

Material	*Composition*	*Thermal shock resistance*	*Thermal conductivity*	*Costs*	*Notes*
Alumina	Al_2O_3	Fair	Low	Low	Most common at high T
Cordierite	$2MgO{\cdot}2Al_2O_3{\cdot}5SiO_2$	Good	Low	Moderate	The lowest thermal expansion
Mullite	$3Al_2O_3{\cdot}SiO_2$	Fair-good	Low	Moderate	Good corrosion resistance
Silicon carbide	SiC	Fair	Low	Moderate high	Does not self-bond easily
Zirconia	ZrO_2	Fair-good	Low	Moderate high	Can be used at temperature >2480K

Ceramic substrates

Alumina is the most commonly used as support
It can be used up to 1500℃
It can alloyed with silica or chromium to improve stregthness

Zirconia is inert to most metals and it can be used at the highest temperature (2210℃)

Cordierite and mullite show a good thermal shock resistance

Substrate

Metallic substrates

Materials:
Stainless steel
Steel alloy (5.5% Al, 22% Cr, 0.5% Co, balance: Fe)
FeCralloy (0.5-12% Al, 20% Cr, 0.1-3% Y, balance: Fe)

The surface of Al-containing alloys is Al-enriched to improve the adherence to the alumina layer

Properties:
Low refractoriness (1670K)
High thermal conductivity
High voidage ➔ lower mass and lower thermal capacity
Faster ignition
Difficult to obtain stable coat of catalyst (especially oxides)

Substrate

Geometric shapes:

Monoliths
Foams
Pellets
Tubes
Fibers
Corrugates sheets

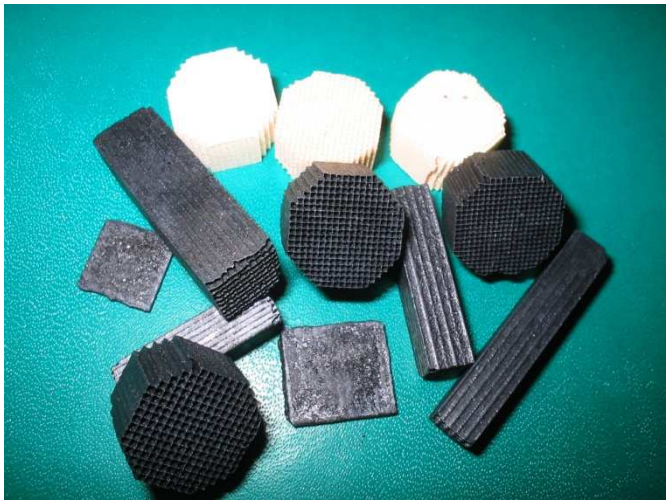

The most common are honeycomb monoliths with parallel channels

Washcoat

Thin layer of a metal oxide material to increase the low surface are of the substrate with a thermal expansion coefficient as close as possible to that of the substrate.

The most common washcoat material: **γ-Al_2O_3**

Problem: phase transition from γ to α at about 900°C with consequent reduction of surface area of two order of magnitude and pores closure with burying of the active phase

⇩

Stabilization of γ-Al_2O_3 with CeO_2, Cs_2O, La_2O_3, BaO ➔ formation of a layer ($LaAlO_3$) which inhibits the surface diffusion of transition aluminas

Use of pre-sintered alumina or ZrO_2 ➔ washcoat with a lower surface area

Active component

The most common active components: Noble metals

Transition metal oxides

Noble metals

Advantages: high specific activity
good resistance to sulphur poisoning

Disadvantages: easy sintering at 500-900℃
volatilization

Noble metals

Ability to activate H_2, O_2 and C-H and O-H bonds

The most active: **Ru, Rh, Pd, Pt** → more active; less volatile; less expensive

Activity Pd>Pt for CO, olefins and methane oxidation
Pt>Pd for paraffins and HC>C_3

Under oxidizing conditions Pd and Pt are well dispersed on alumina surface as oxides.

At $T>T_{decomposition}$ Metal oxide➔metal Formation of large metallic particle

(T=585℃ for PtO_2; T=790℃ for PdO)

The strong interaction between Pd and alumina provides a catalyst with a good thermal stability

Transition metal oxides

The most active: **Cr_2O_3, NiO, CuO, MnO_x**

Activity related to multiple valence states

Advantages: less expensive
less volatile

Disadvantages: lower activity
higher light off T
formation of less active spinels (interaction with the support)

Problem: formation of surface spinels at high temperature due to the interaction with alumina ➔ activity of spinel < activity of the corresponding simple oxide

Mixed oxides have a higher thermal stability ➔ higher melting point (sintering occurs at T=1/3 $T_{melting}$)

Other oxides

Hexaaluminates: $MO:6Al_2O_3$ (M=Ba, Sr, Ca)

Substitued hexaaluminates: $M(M_2)x\ Al_{11-x}O_{19-y}$) ($M_2$=Cr, Mn, Fe, Co+Ni)

Advantages: high thermal stability (presence of M promoting the formation of a layered aluminate structure)

Disadvantages: low activity (increased by the substitution with a transition metal cation)

Other oxides

Perovskites: **ABO_3 (A = rare earth cation, B= transition metal cation)**

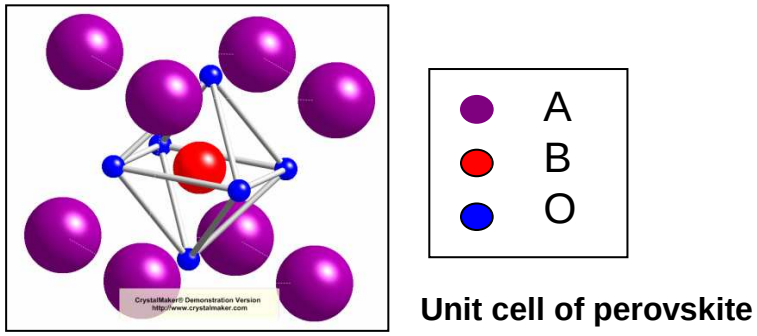

Unit cell of perovskite

Advantages: good thermal stability
Activity comparable to that of noble metals (Mn and Co most active cations)

Disadvantages: sintering at high temperature
possible interaction between transition metal cation and the support

Perovskites

High chemical stability: perovskite structure can be formed provided that *tolerance factor* t is in the range 0.8-1.

$$t=(R_A+R_O)/\sqrt{2}\,(R_B+R_O)$$

Non-stoichiometry: presence of anionic or cationic vacancies (present in the original material or induced by partial cation substitution)

⇩

High oxygen mobility: adsorption and desorption of large amount of oxygen

Catalysts preparation

Coating of washcoat layer

Preparation of a sol

Hydrolysis of the alkoxide

$$M(OR)_n + nH_2O \rightarrow M(OH)n + nROH \qquad M=Al, Si, Ti, Zr$$

During the hydrolysis, generally accelerated by the addition of an acid or a base, polycondensation takes place (cross-linking with formation of a polymer like compound)

$$-M\text{-}OH + HO\text{-}M' \rightarrow -M\text{-}O\text{-}M' + H_2O$$

Coating of washcoat layer

Procedure

- Dipping of the structured substrate into the sol.
- Removing of the remaining sol (blow off)
- Drying
- Calcination

Washcoating of metallic substrate is more difficult than that of ceramic substrates. A preliminary oxidation of the metallic substrate improves the washcoat adhesion

Deposition of active species

- **Impregnation** (*dipping of monolith in a solution containing precursors of the active phase)*
  very simple
  possible not homogeneous distribution

- **Adsorption and ion exchange** (*precursors species are exchanged with the surface group of the surface of the oxide layer)*
  low amount of active phase
  more homogeneous distribution

- **Precipitation and co-precipitation** (*addition to the impregnation solution of a precipitation agent, as hydroxide)*
  high amount of active phase
  weak adhesion of the precipitated particles to the washcoat

- **Deposition-precipitation** (*addition of an agent which slowly decomposes, as urea, increasing pH and leading to hydroxide precipitation)*
  more homogeneous distribution compared to precipitation

- **Sol-gel method** (*the active phase is encapsulated in the oxide layer by adding the precursor in the sol for the washcoat)*
  used for less expensive active phase

Catalysts characterization

- Mechanical
- Morphological
- Physical
- Chemical

Mechanical characterization

Tests of adhesion of the washcoat layer with ultrasounds

(generally coupled to gravimetric analysis or SEM analysis of the structured catalyst)

Expansion/contraction of the reactor during the start-up/start-down

Morphological characterization

SEM analysis: *scanning of the sample surface with a high energy electron beam*

Evaluation of inner channel coating, estimation of the washcoat thickness, detection of big agglomerates.

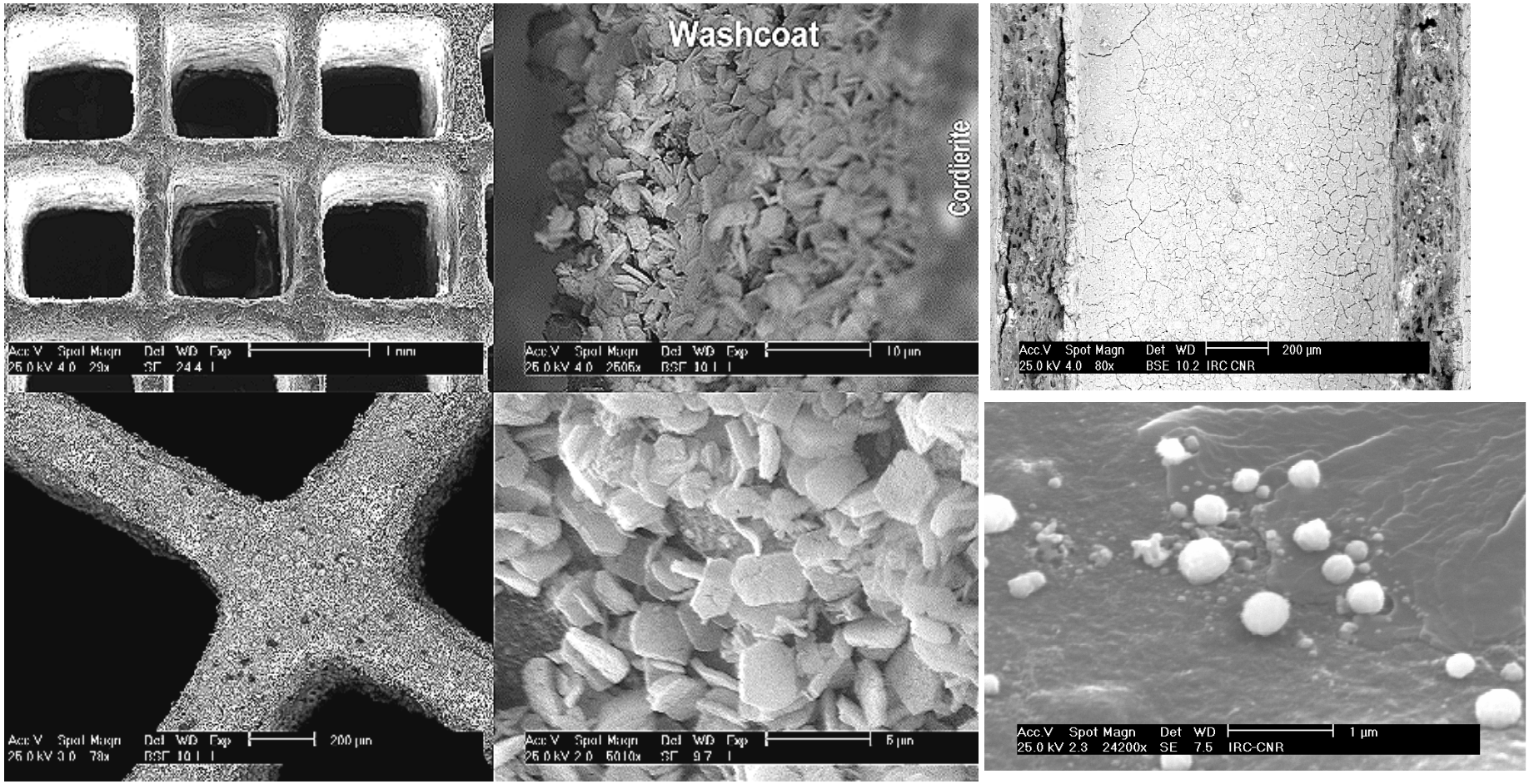

SEM coupled to EDAX: local or average surface composition and distribution of elements.

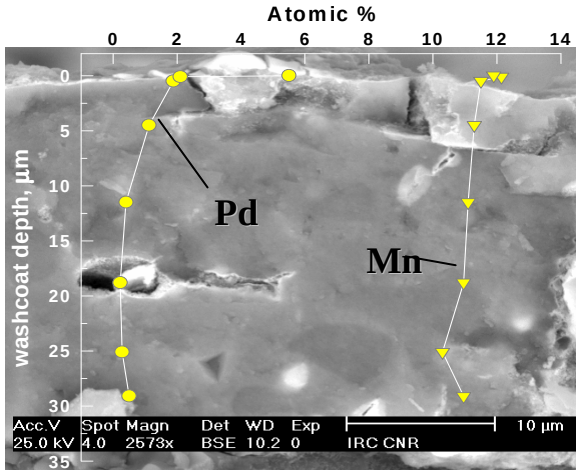

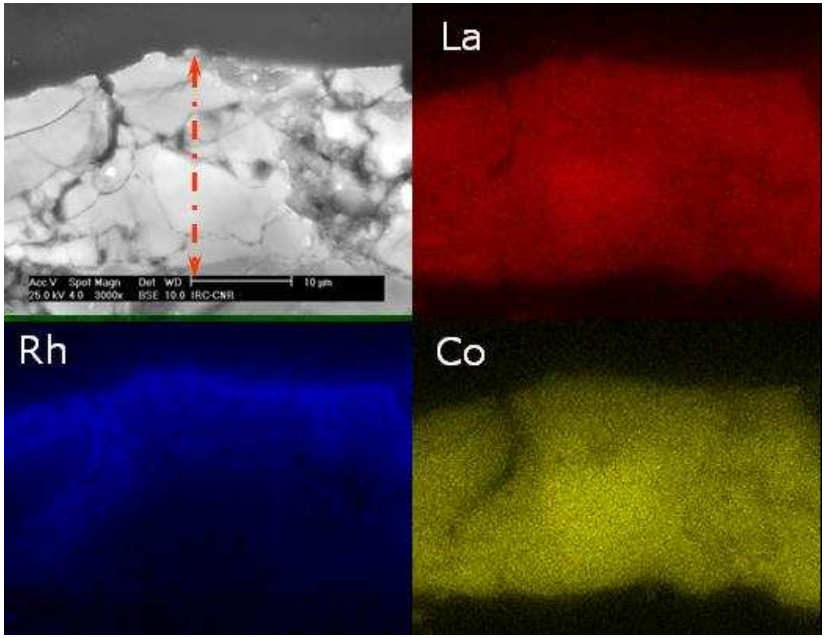

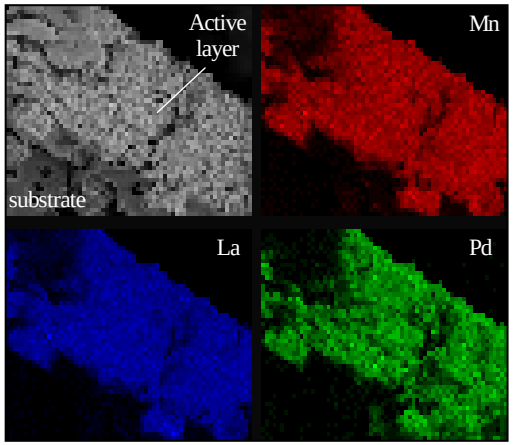

Physical characterization

BET analysis: *N_2 adsorption at 77K*
Evaluation of surface area
(≠geometrical area) based on:

$$\frac{P}{V(P_O - P)} = \frac{1}{V_m C} + \frac{(C-1)}{V_m C}\frac{P}{P_O}$$

P= gas pressure
Po= saturated vapour pressure of the liquid at the experimental temperature
V= amount of gas adsorbed
Vm= amount of gas required to cover the surface to one monolayer thickness
C= constant

Linearization of this equation allows the estimation of the surface area S:

S= specific surface area (m^2g^{-1})
Na= Avogadro's number
Am= area of N_2
Vo= volume of 1 mol STP
W= catalyst weight (g)

$$S = \frac{V_m A_m N_a}{W V_o}$$

Physical characterization

Porosity: *N_2 adsorption+desorption at 77K, mercury porosimetry*

Evaluation of pore size distribution, pores volume, mean pore radius.

Adsorption+desorption curves indicate the type of porosity (slope, presence of hysteresis due to capillary condensation into mesopores)

Micropores ϕ<2nm

Mesopores 2<ϕ<50nm

Macropores ϕ>50nm

The most common for mesopores: Kelvin equation

$$r_K = \frac{2\sigma V \nu_1}{RT \ln(p / p_o)}$$

r_K= Kelvin radius

σ= surface tension of the condensate liquid

ν1= molar volume

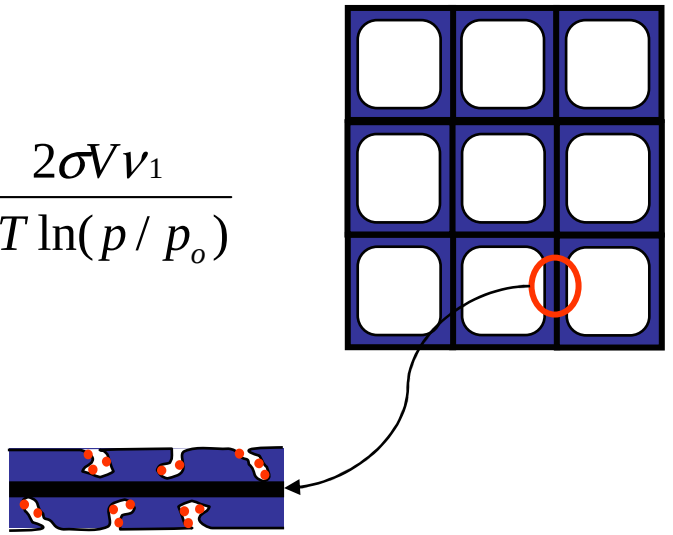

Mercury porosimetry for macropores and mesopores range

Physical characterization

Metallic surface area

Evaluation of metal dispersion by selective chemi-sorption on reduced metal sites of different molecules (H_2, CO, O_2, N_2O etc.)

Static methods: determination of monolayer uptake by pressure measure at adsorption equilibrium at additional gas dosing
Dynamic methods: determination of monolayer uptake in adsorbate gas flow

Correct choice of adsorbate gas ➔ *adsorption stoichiometry*

Multiple stoichiometry
Spill-over effect
Formation of hydride

Physical characterization

XRD analysis

Evaluation of crystalline phase, evaluation of crystallite mean size (Scherrer formula), determination of possible phase transition.

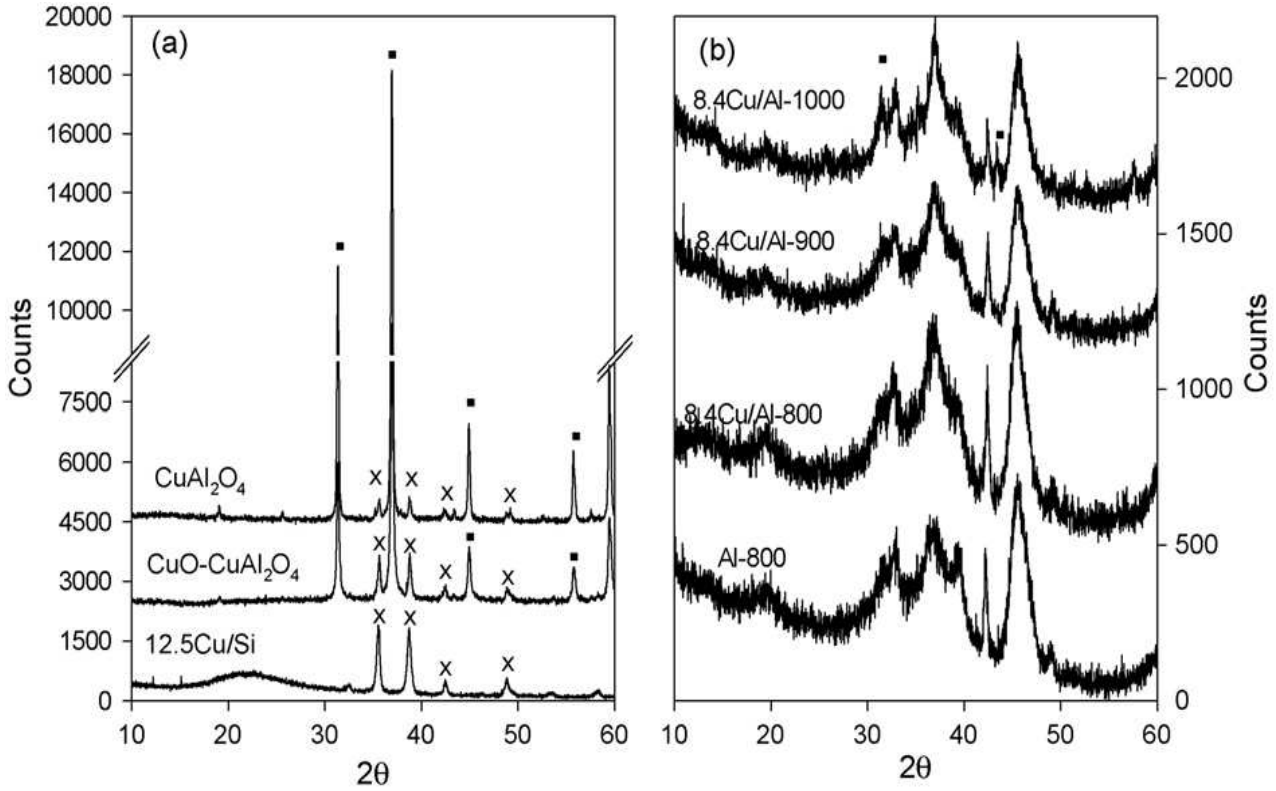

Chemical characterization

Atomic absorption-ICP analysis

Evaluation of type and concentration of active elements based on the emission of each element at a specific wavelength.

Evaluation of the total concentration of the active element

Chemical characterization

Thermochemical analysis

Thermogravimetry

Temperature Programmed Reduction/Oxidation/Desorption

Evaluation of the thermal behaviour of the catalyst under different mixtures (reducing, oxidative, reaction) or using probe molecules (acid/basic properties)

$$MO_n + nH_2 \rightarrow M + nH_2O$$

$$MO_n + nCO \rightarrow M + nCO_2$$

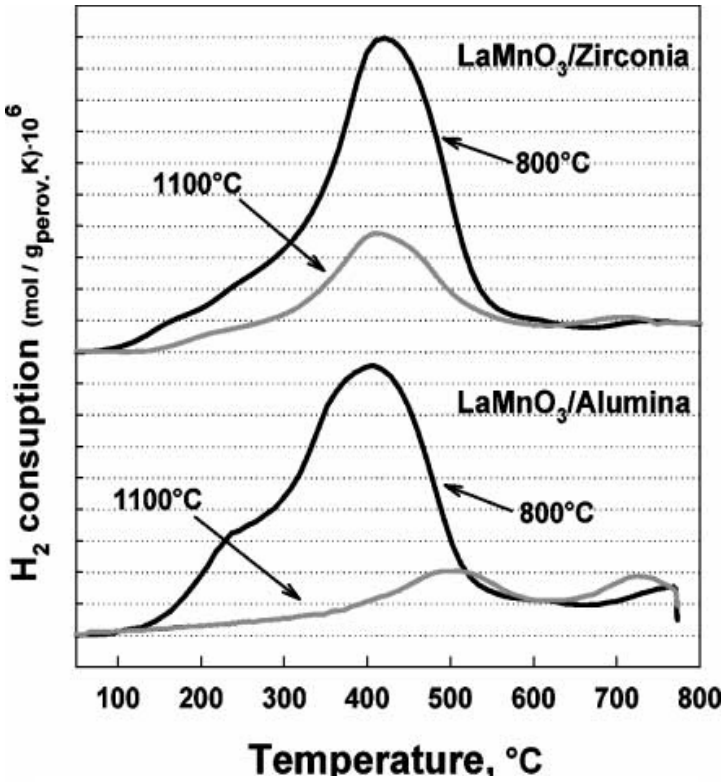

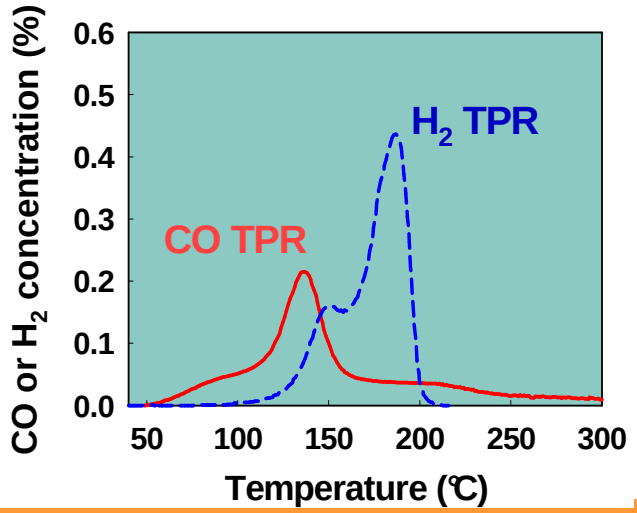

Chemical characterization

FTIR spectroscopy

Evaluation of the nature of active sites through adsorption of probe molecules (CO, NO, ammonia, pyridine).

Transmission: some of the IR radiation is absorbed by the sample and some is passed through (transmitted)

internal and external transport limitations

limited to the analysis of samples transparent to IR radiation

self-supported pellets

DRIFT: the angle of reflection is different from the angle of incidence

no transport limitations (powder)

samples with bad IR transmission or with a strong scattering

In-situ spectroscopy

In-situ
transmission cell

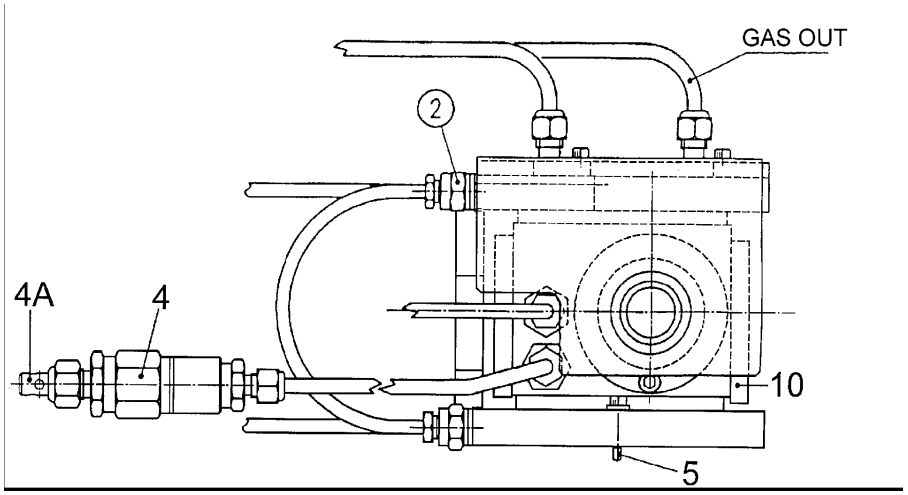

Assembly of cell reactor in transmission mode: 1) ZnSe window; 2) water cooling connectors; 3) inlet gas; 4) pressure burst disc attachment; 5) cooling plates.

Heat
Chamber

In-situ DRIFT cell

Sample
Cup

ZnSe
Window

Chemical characterization

FTIR spectroscopy coupled to TGA

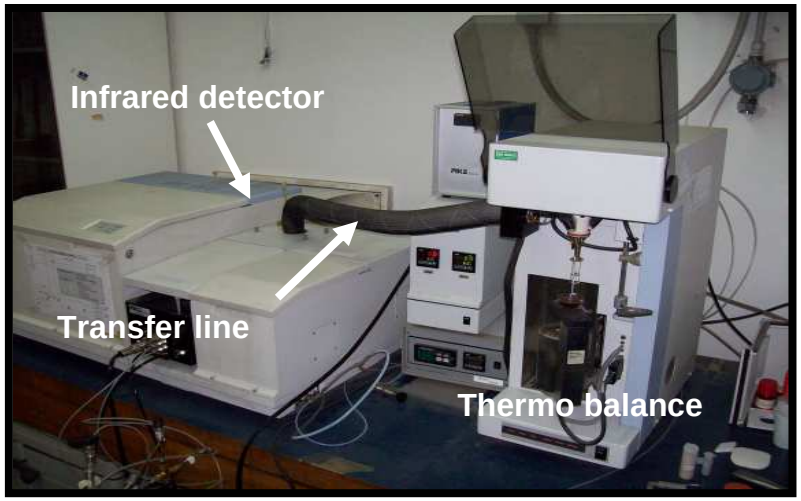

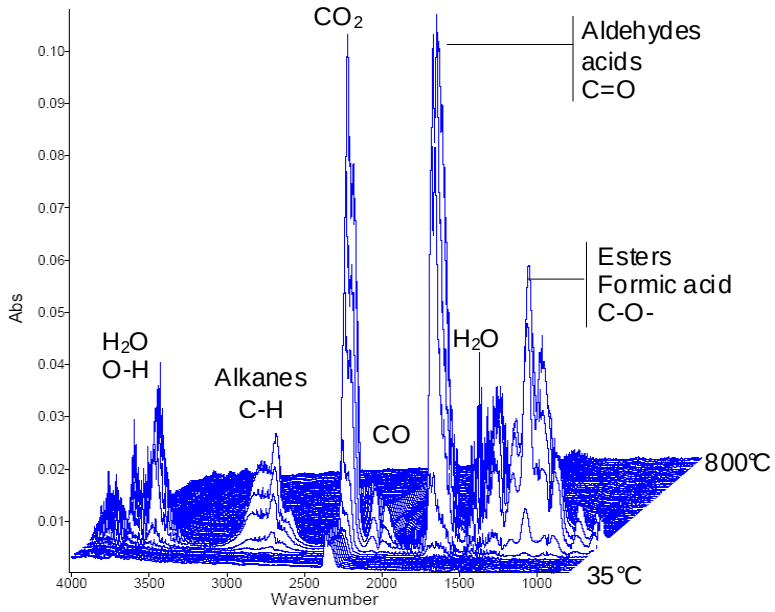

Gaseous and volatiles species from biomass decomposition

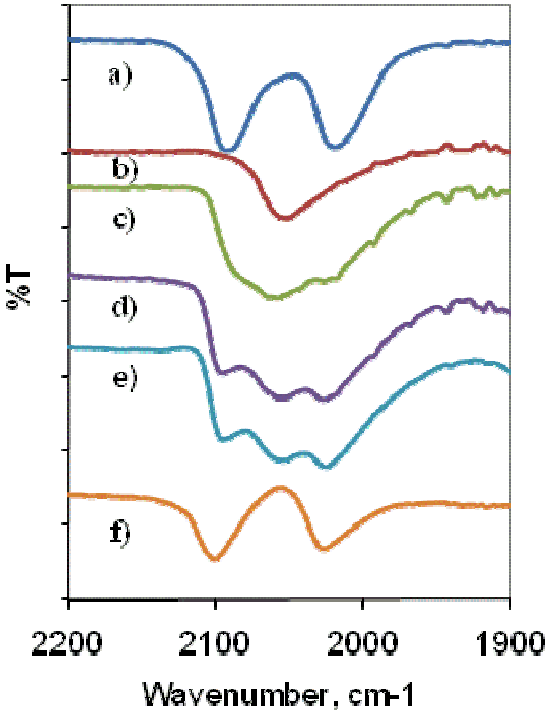

In-situ CO adsorption on Rh sites under S-containing or not gas mixture at different temperatures

Rh/Al_2O_3 catalyst

Chemical characterization

X-ray Photoelectron Spectroscopy (XPS)

Identification of surface elements, evaluation of their concentration and oxidation state and compounds through the measure of the binding energy

Surface composition of the catalysts (about 10nm)

$Pd/LaMnO_3$ based catalyst

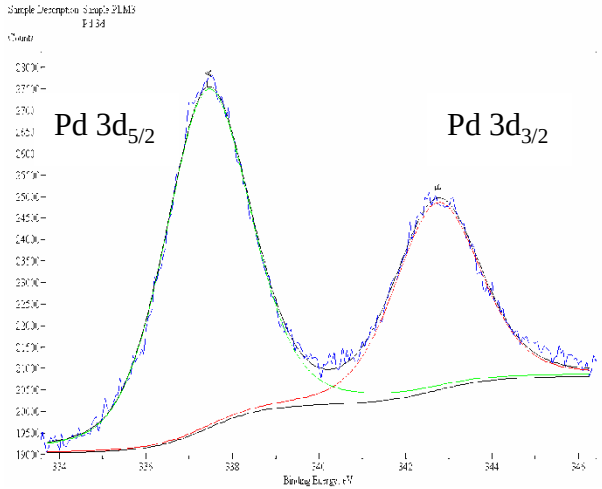

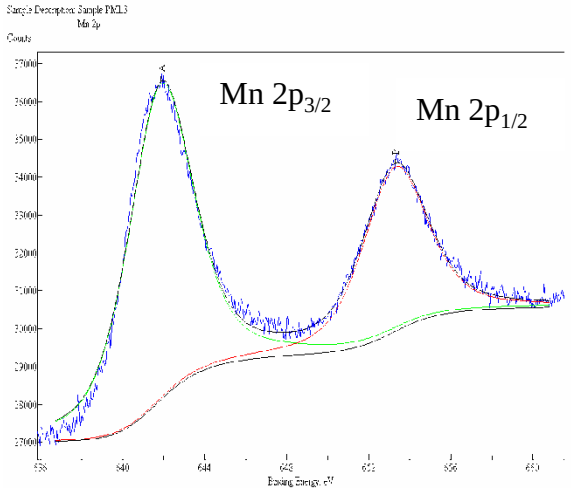

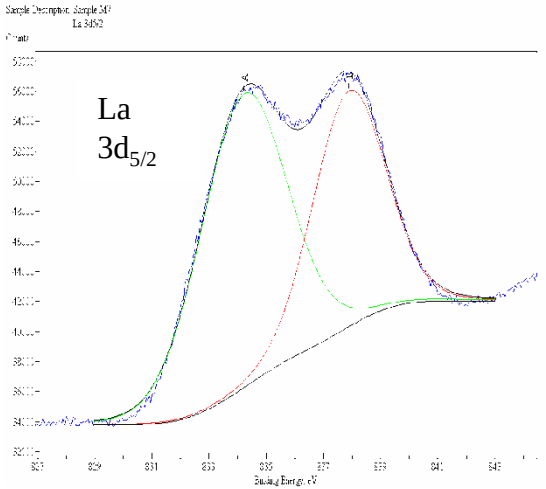

Peak	Mean BE (eV)	Assignment
Pd $3d_{5/2}$ (A)	337.2	Pd^{2+} as in PdO
Pd $3d_{5/2}$ (C)	338.6	Pd^{4+} as in PdO_2

Peak	Mean BE (eV)	Assignment
Mn $2p_{3/2}$	641.7	Mn^{3+} as in Mn_2O_3
La $3d_{5/2}$	834.0	La^{3+} as in La_2O_3

Palladium: surface concentration and distribution of Pd species in the fresh and used catalysts

Catalyst	Surface Pd content (wt %)	Pd species distribution (%)		
		Pd^0	Pd^{2+}	Pd^{4+}
P1LM (fresh)	1.1	6.8	87.0	6.2
P1LM (act.)	0.3	14.9	78.1	7.0
P3LM (fresh)	7.5	1.9	81.7	16.4
P3LM (act.)	2.4	9.2	86.0	4.8

References:

R. Praasad, L. A. Kennedy, E. Ruckenstein, **Catalytic combustion**, Catal. Rev. – Sci. Eng. 26 (1984) 1.

L. D. Pfefferle, W. C. Pfefferle, **Catalysis in combustion**, Catal. Rev. – Sci. Eng. 29 (1987) 219.

M. F. M. Zwinkels, S. G. Järås, P. G. Menon, **Catalytic fuel combustion in honeycomb monolith reactors**, in Structured Catalysts and Reactors, A. Cybulsky and J. A. Moulijn Eds. (1998).

K. Eguchi, H. Arai, **Recent advances in high temperature catalytic combustion**, Catal. Today 29 (1996) 379.

A. Cybulsky and J. A. Moulijn, **Monoliths in heterogenous catalysis**, Catal. Rev. – Sci. Eng. 36 (1994) 179.

L. Tejuca, J. L. G. Fierro, J. M. D. Tascòn, **Structure and reactivity of perovskite-type oxides**, Advances in catalysis, 36 (1989) 237.

Handbook of heterogeneous catalysis, G. Ertl, H. Knözinger, J. Weitkamp Eds. (1997), vol. 2

Summary

Characterization of fluidodynamic behaviour of catalyst

Comminution phenomena of catalyst particles

- primary fragmentation
- attrition
- elutriation
- experimental apparatus for their determination

Influence of preparation method on shape and mechanical resistance of a system

- rotating pan granulation
- gas phase granulation (spray dry)
- drop coagulation: sol gel method (oil and hydrocarbon-ammonia molding)
- a new technology for the production of γ-alumina

Influence of the comminution phenomena on the choice and applicability of a catalyst in a fluidized bed reactor: some study case

- Developing of a catalyst for catalytic methane combustion in fluidized bed
- Catalyst for biomass gasification process
- Developing of oxygen carrier for chemical looping combustion

Attrition as suitable method for catalyst regeneration: catalytic methane decomposition process (TCD)

Characterization of fluidodynamic behaviour of catalyst

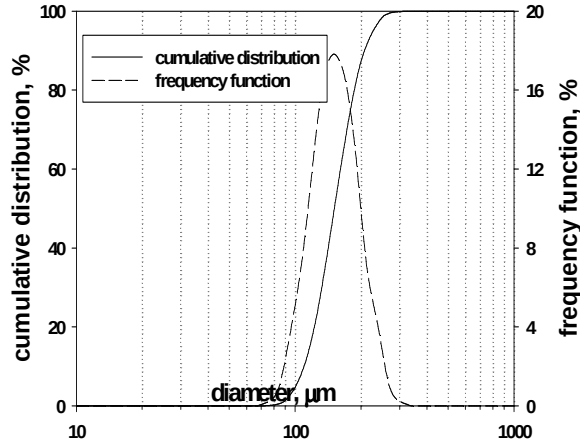

Size distribution

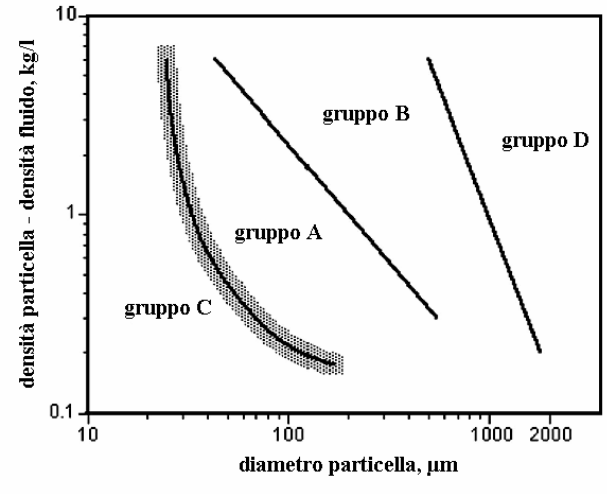

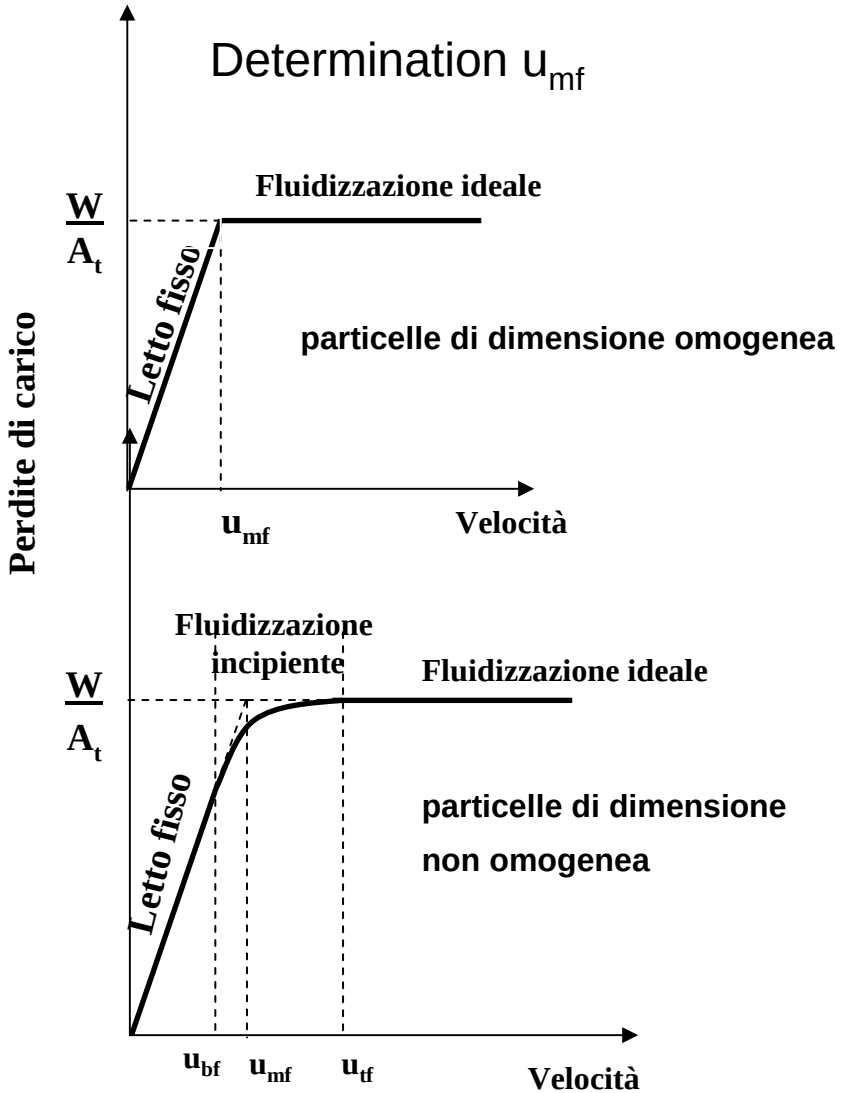

Comminution phenomena

Comminution phenomena of fuel particles

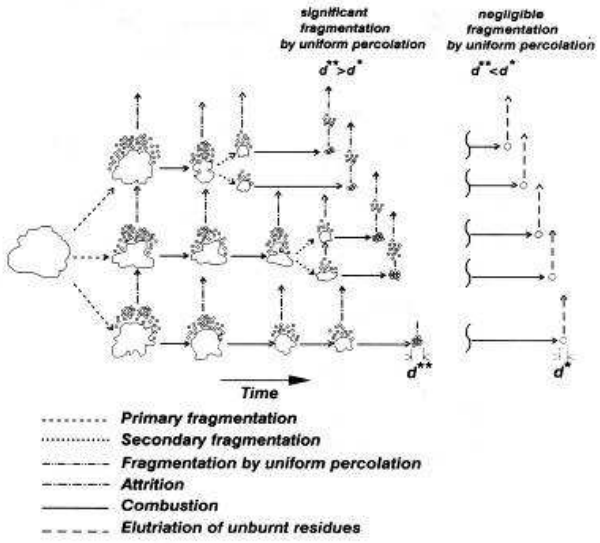

Comminution phenomena of catalyst particles

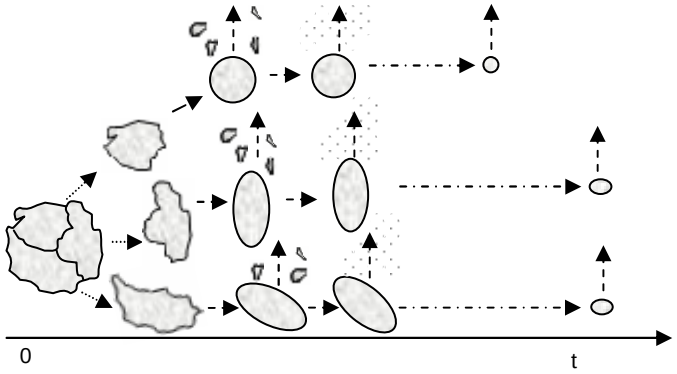

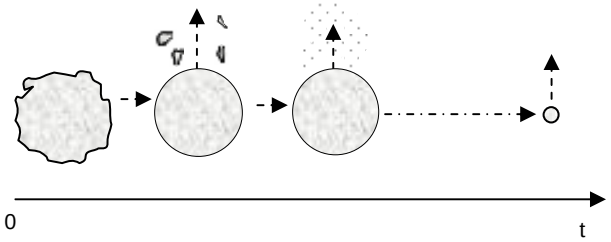

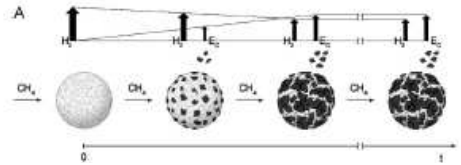

Experimental apparatus for the characterization of comminution phenomena

basket equipped FB

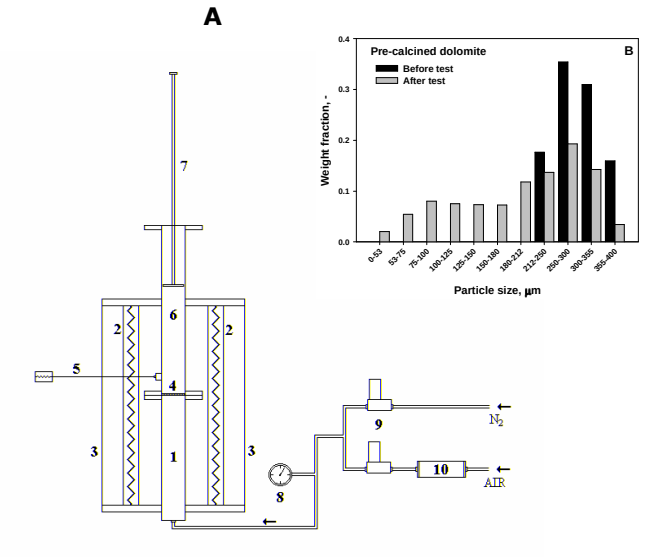

1) gas preheating section; 2) electrical furnaces; 3) ceramic insulator; 4) gas distributor; 5) thermocouple; 6) fluidization column; 7) steel basket; 8) manometer; 9) digital mass flowmeters; 10) air dehumidifier (silica gel).

two-exit head FB

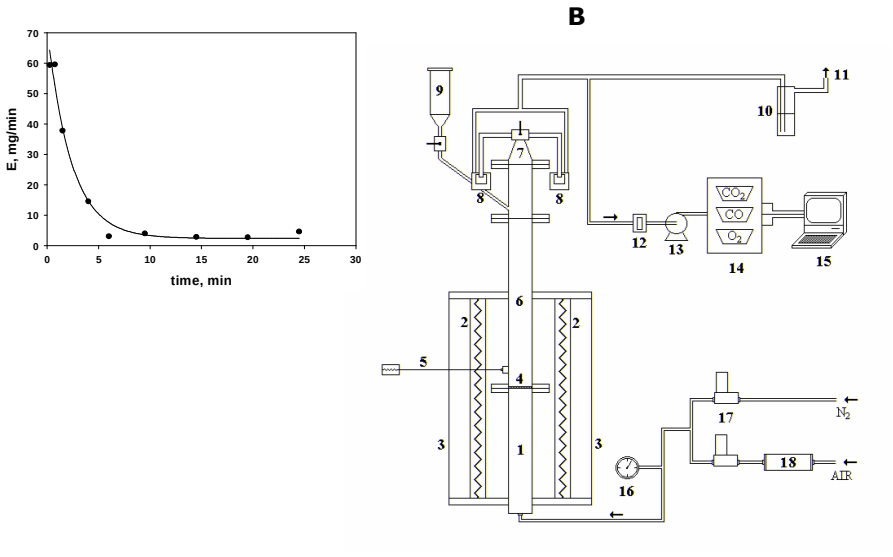

1) gas preheating section; 2) electrical furnaces; 3) ceramic insulator; 4) gas distributor; 5) thermocouple; 6) fluidization column; 7) head with three-way valve; 8) sintered brass filters; 9) hopper; 10) SO_2 scrubber; 11) stack; 12) cellulose filter; 13) membrane pump; 14) gas analyzers; 15) personal computer; 16) manometer; 17) digital mass flowmeters ; 18) air dehumidifier (silica gel).

Influence of preparation method on shape and mechanical resistance of a system

Spherical shape more suitable for use in fluidized bed

Shape	Size
Extrudate	$d = 1–50$ mm $l = 3–30$ mm
Pellet	$d = 3–15$ mm $h = 3–15$ mm
Granule, Bead	$d = 1–20$ mm $d = 1–5$ mm
Sphere	$d = 1–10$ mm
Microspheroidal	$d = 20–100$ μm

Perego C. and Villa P. L. 1997

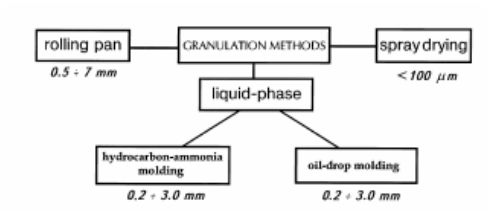

Z.R. Ismagilov*, R.A. Shkrabina, N.A. Koryabkina
Catalysis Today 47 (1999) 51–71

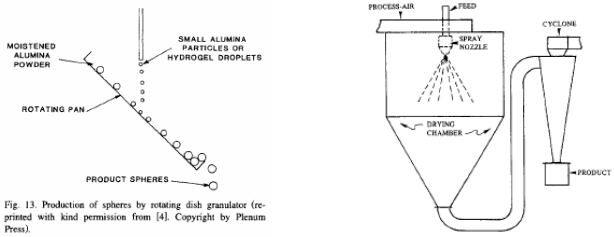

Fig. 13. Production of spheres by rotating dish granulator (reprinted with kind permission from [4]. Copyright by Plenum Press).

Perego C. and Villa P. L. 1997

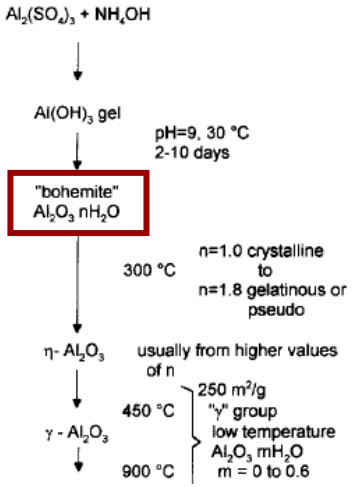

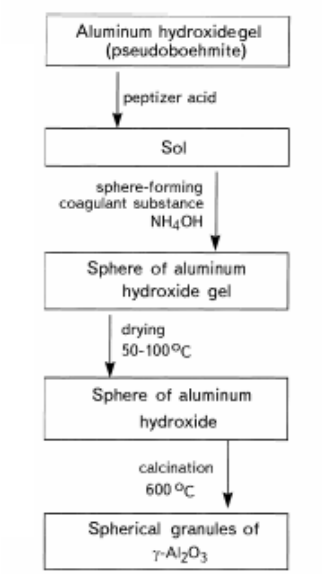

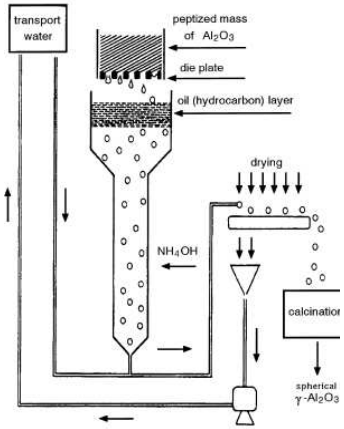

Perego C. and Villa P. L. 1997

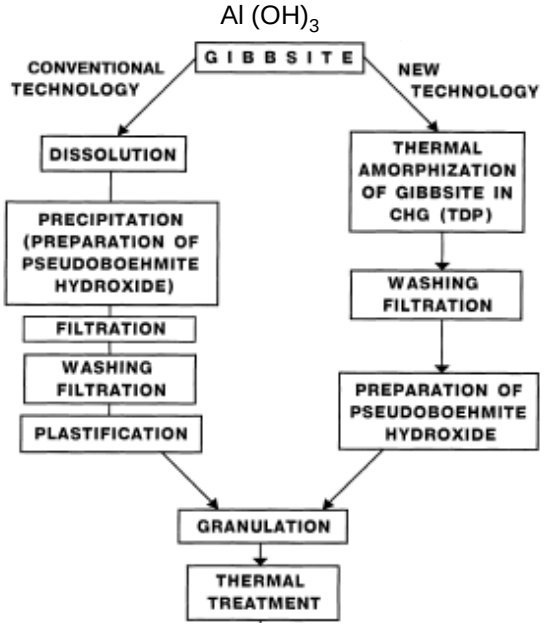

Z.R. Ismagilov*, R.A. Shkrabina, N.A. Koryabkina
Catalysis Today 47 (1999) 51–71

Influence of the comminution phenomena on the choice and applicability of a catalyst in a fluidized bed reactor

Catalytic combustion

Lower temperatures than in conventional flames ⇒ Thermal NO_x control

Air/fuel mixtures outside flammability limits ⇒ Safer applications, VOC combustion

Low efficiency in heat removal from catalytic surface ⇒ Catalyst thermal deactivation

Catalytic combustion in Fluidized Bed

Efficient heat transfer due to conduction ⇒ Lower catalyst temperatures ⇒ Prevention of thermal deactivation

- Unconverted fuel by-pass in bubble phase must be avoided in order to reach complete fuel conversion
- Possible loss of catalyst due to comminution phenomena

Developing of a catalyst for methane catalytic combustion in fluidized bed

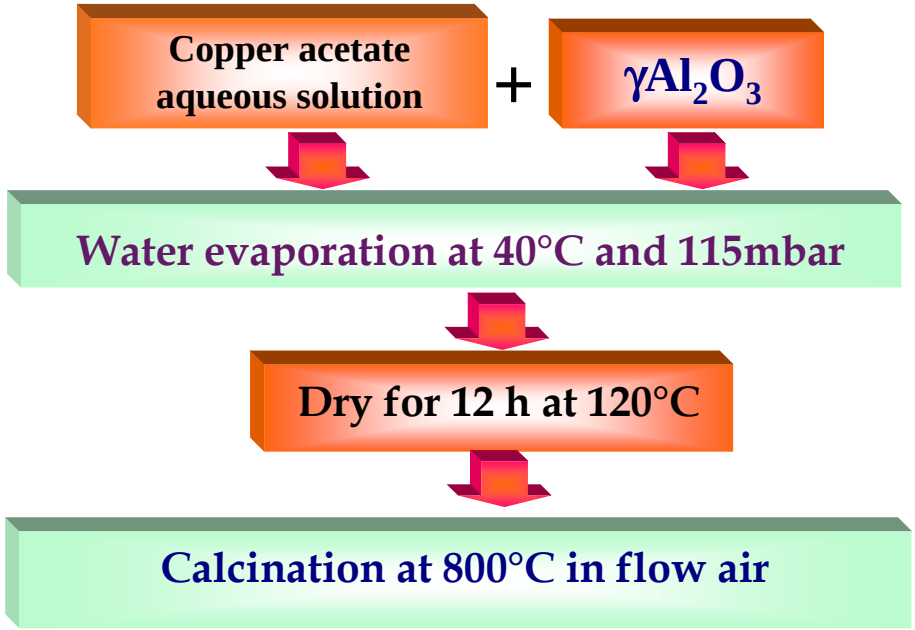

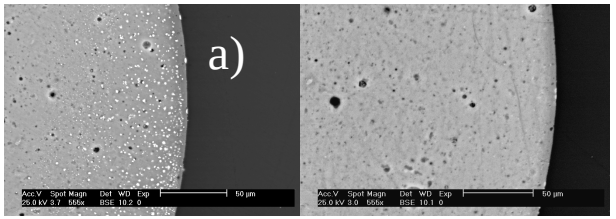

Particles size: 1μm
Density: 1.8g/cm³

Active phase : surface $CuAl_2O_4$

%Cu (%wt)	Surface area (m^2/g)
5.5	144

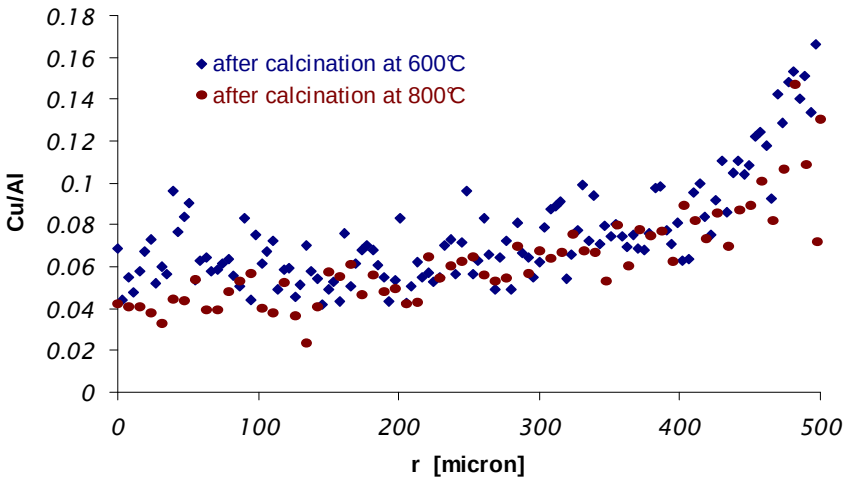

Iamarino et al. 2002

Characterization of fluidization properties of the catalyst

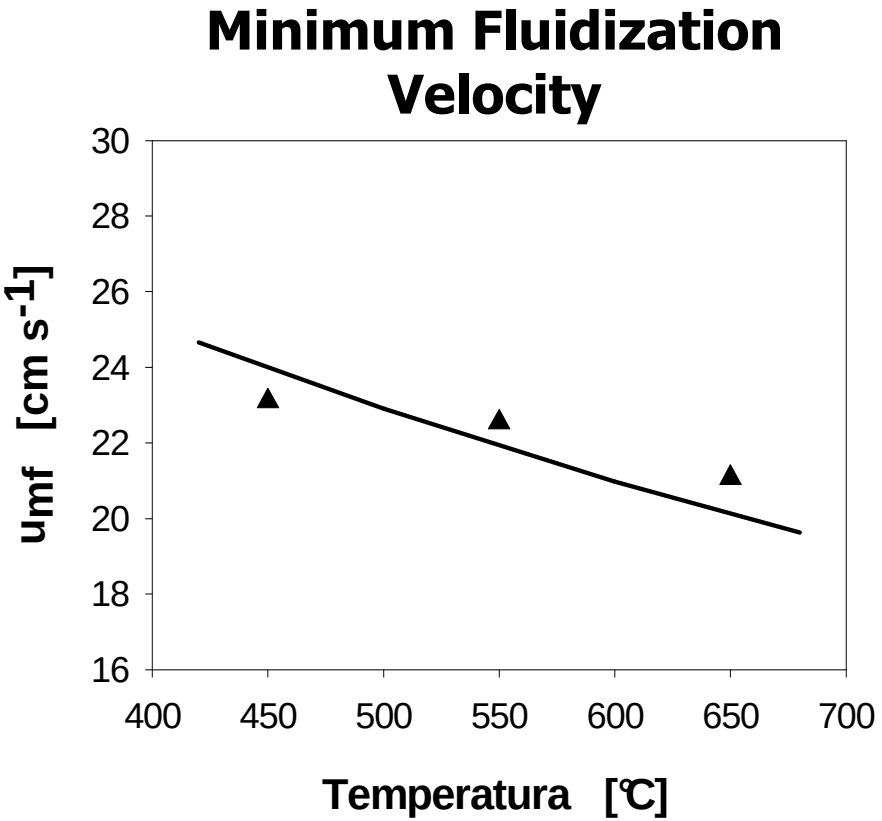

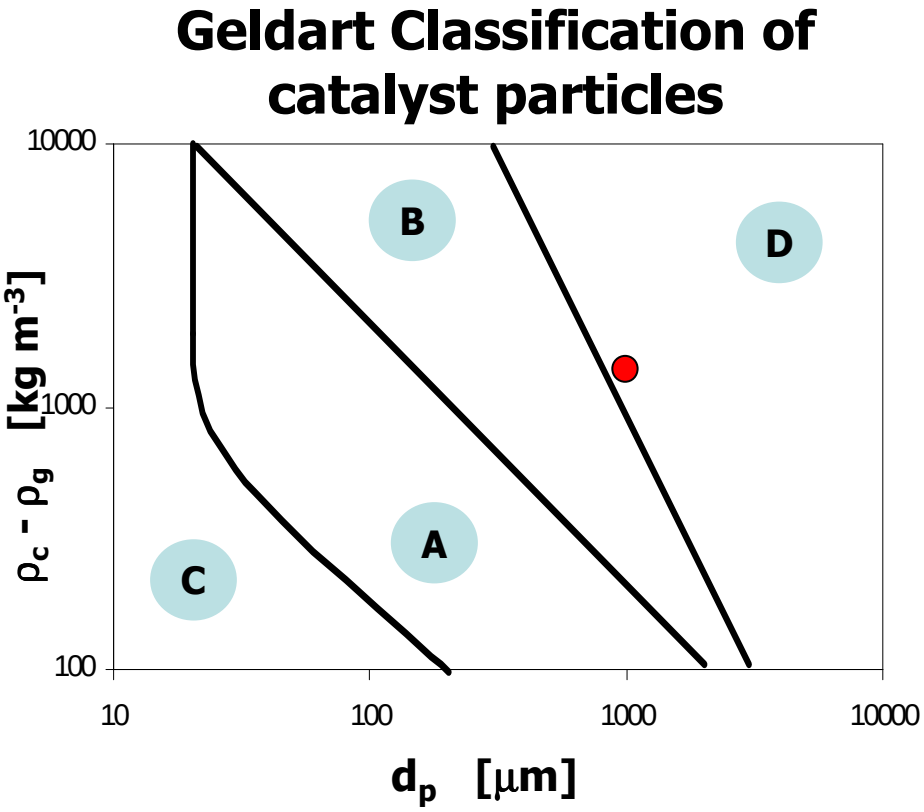

Geldart , 1986

$$\frac{D_p v_{mf} \rho_g}{\mu} = [(33.7)^2 + 0.0408 Ar]^{0.5} - 33.7$$

$$Ar_{p,mf} = \frac{D_p^3 \rho_g (\rho_s - \rho_g) g}{\mu^2}$$

Wen, C.Y. And Y.H. Yu, 1966

Characterization of comminution phenomena

No primary fragmentation is observed for the catalyst

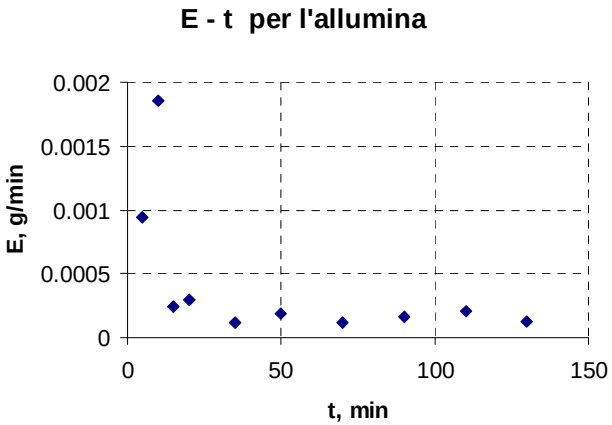

$K=5.6*10^{-7}\ min^{-1}$

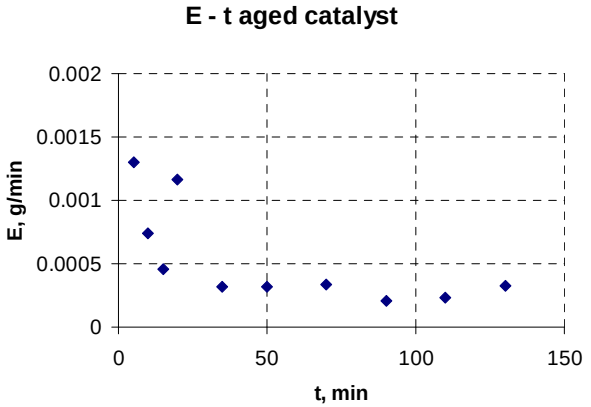

$K=1.7*10^{-6}\ min^{-1}$

Fines Elutriation Rate at Different Superficial Velocities

u_0 [m s^{-1}]	elutriation rate [g h^{-1}]
0.4	not detectable
0.6	0.3
0.8	1.6
1.0	4.5

Iamarino et al. 2006

$$\mathbf{Ec = Ka(u-u_{mf})*W_{cat}/D_p}$$

Some results

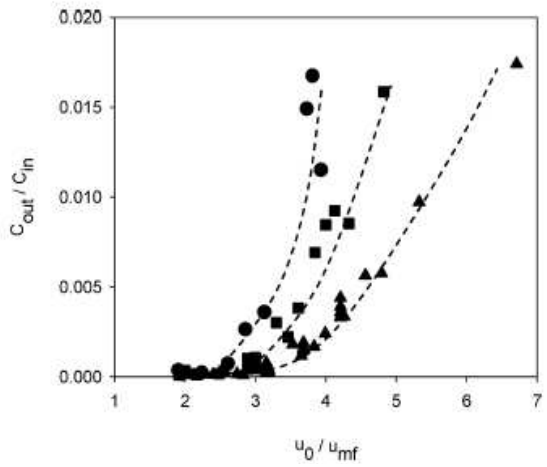

C_{out}/C_{in} as a function of u_0/u_{mf} at temperatures of 650 (●), 700 (■), and 750 ℃ (▲). For each temperature, data correspond to inlet methane concentrations in the range **4-9 vol** %.

Iamarino et al. 2006

No CO formation

High methane conversion also for
High inlet concentration
Thermal power 4.5kW at 750 C →

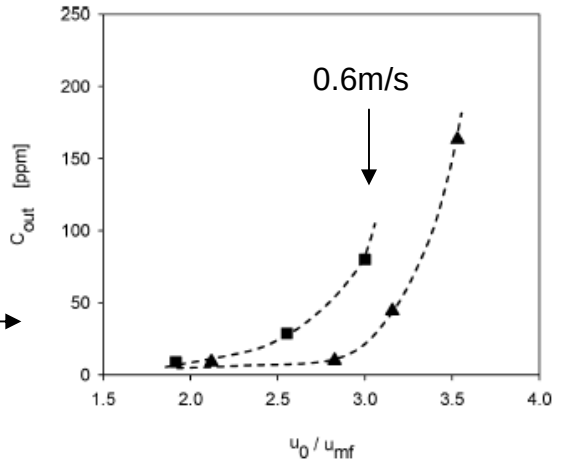

Outlet methane concentration [ppm] at high conversion degrees (C_{in}= 9 vol %, T= 700 (■) and 750 ℃ (▲)).

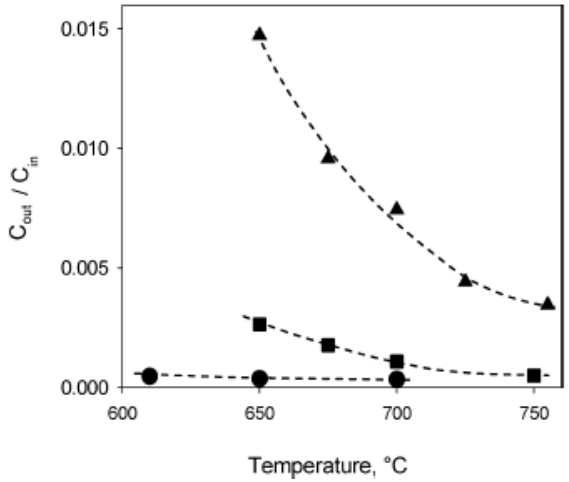

Normalized outlet methane concentration at C_{in} = 6 vol % and u_0 =0.40 (●), 0.60 (■), and 0.80 (▲) m s^{-1}.

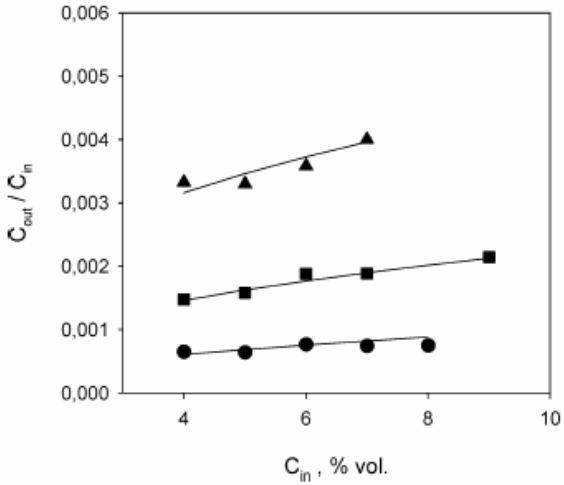

Effect of methane inlet concentration on C_{out}/C_{in} at T = 750 ℃ and u_0 = 0.60 (●), 0.70 (■), and 0.80 (▲) m s^{-1}.

Biomass gasification

One of the best way to optimize the extraction of energy from biomass and to obtain a standardized gas starting from very different materials

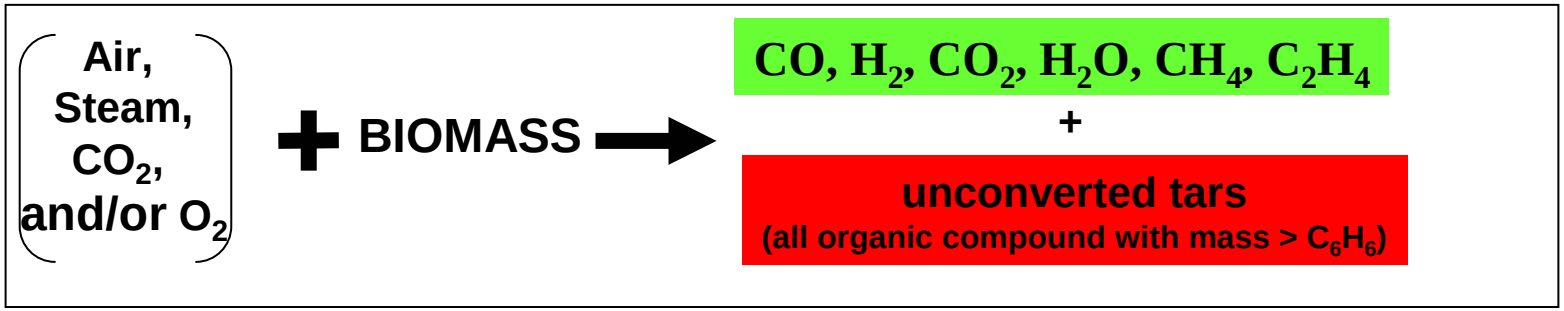

Low Calorific Value:	4 - 6 MJ/Nm^3	Using air and steam/air
Medium Calorific Value:	12 - 18 MJ/Nm^3	Using oxygen and steam

The main challenges of biomass gasification are:

- **Good control of temperature in the reactor**
  - High heating rate (hundreds of degrees per second) and high temperatures (around 800°C) are necessary to maximize the gas yield
- **TARS conversion**
  - TARs condense in the cold parts ⇒ plugging of tubes or agglomeration phenomena
  - TARS removal by filtration ⇒ lost of efficiency since they still contain energy

Catalytic biomass gasification in fluidized bed

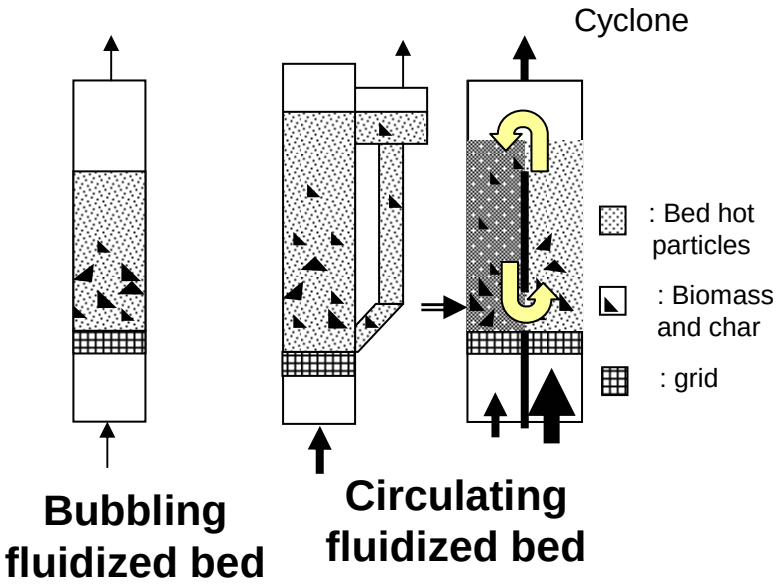

Advantages:

uniform temperatures and high heating rates, greater tolerance to particle size range

Drawbacks:

low density biomass fuel (with respect to the bed particles) segregates to the surface of the bed reducing the conversion rate.

Fine carbon particles produced in the reaction process elutriate (increasing the solid load to the cyclone and the filter).

Fused ash and tar condensation provokes defluidization.

The catalytic tars conversion can both decrease tar production and modify gas composition.

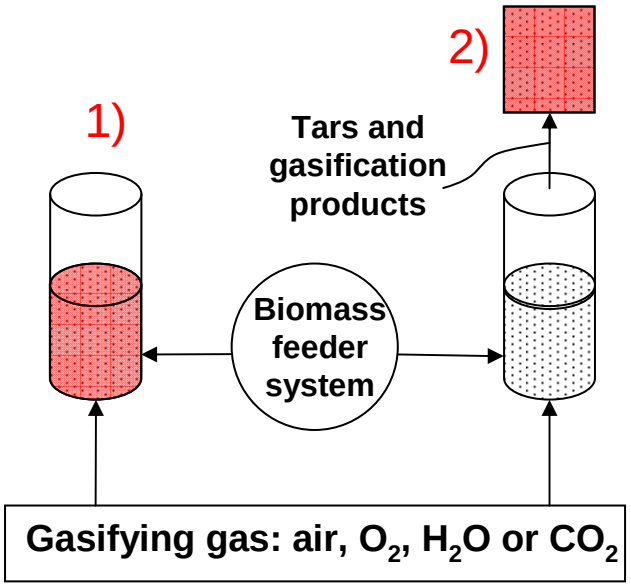

There are two ways for catalytic tar removal:

1: Primary method: the catalyst is mixed with biomass directly inside the gasifier.

Single-stage process

2: Secondary method: the catalyst is placed down stream the gasifier.

Dual-stage process

Catalyst for biomass gasification process

Characterization of primary fragmentation

Both fresh and pre-calcined dolomite undergo extensive fragmentation (mass of fragments of the order of 50-60% by weight).

Fragmentation is mostly caused by the thermal/mechanical shock rather than by the CO_2 release, since for the pre-calcined sample the latter does not occur during the test.

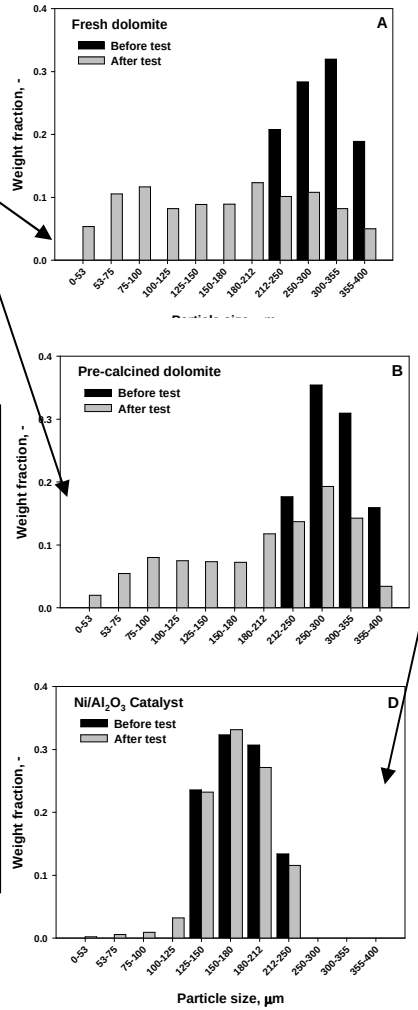

The alumina catalyst particles appear to be very resistant to thermal-mechanical fragmentation

The particle size distributions before and after the test are almost equal.

Sauter mean diameter of the samples before and after fragmentation experiments

	Before test (mm)	***After test (mm)***
Fresh dolomite	**0.293**	**0.114**
Pre-calcined dolomite	**0.292**	**0.152**
Ni/Al_2O_3 catalyst	**0.172**	**0.162**

Catalyst for biomass gasification process

Characterization of attrition

The initial higher fines generation is due to the rounding off of the rough particles by mechanical removal of surface asperities.

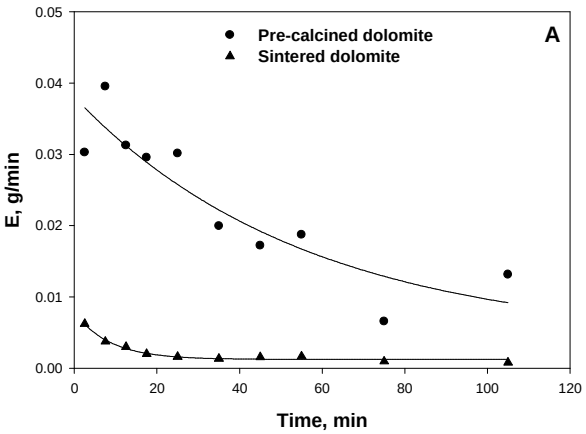

Consistently with the fragmentation results, the pre-calcined dolomite shows a larger fines elutriation rate, indicating that this material is more fragile than the other.

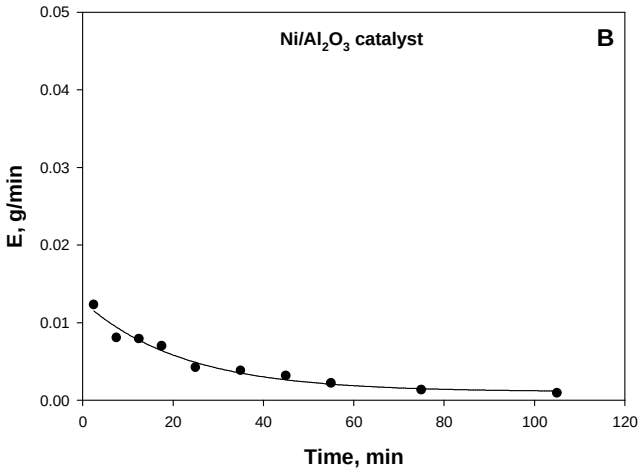

catalyst particles appear to have a relatively good resistance to attrition.

Fillite a new support for biomass gasification catalytic process in fluidized bed?

Trelleborg Italia provided us the cenospheres. Patent name “Fillite 300A”

Average particle density	**700-900 kg·m^{-3}**
Shell hardness	**Mohs scale 6**
Crush strength	**140-280 kg·cm^{-2}**

Low density suitable to prevent starting segregation phenomena

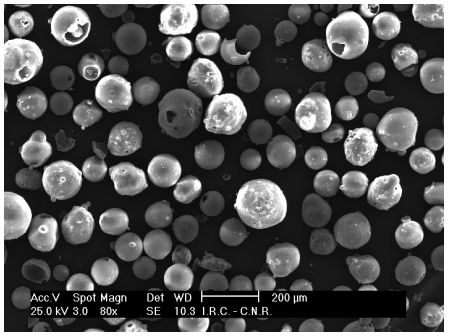

XRD Analysis

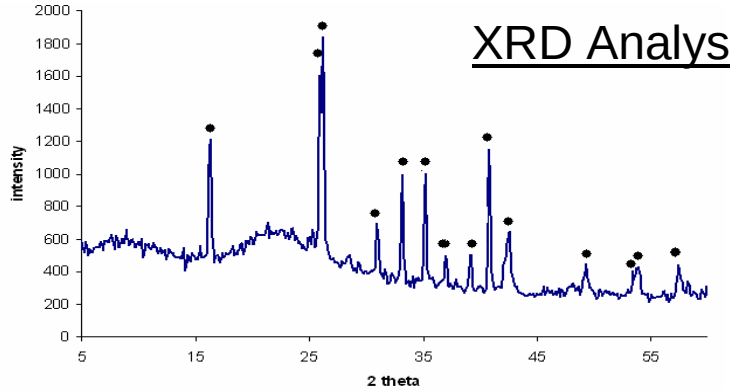

EDX Analysis

Elements	Na	Al	Si	K	Ca	Ti	Fe
weight percent	**1,04**	**33,25**	**59,51**	**0,98**	**0,39**	**3,25**	**1,58**

Internal surface of a half-cut particle

Characterization of fluidization properties of fillite

cenospheres material in the size range 125-212 μm in Air.

Granulometric Analysis

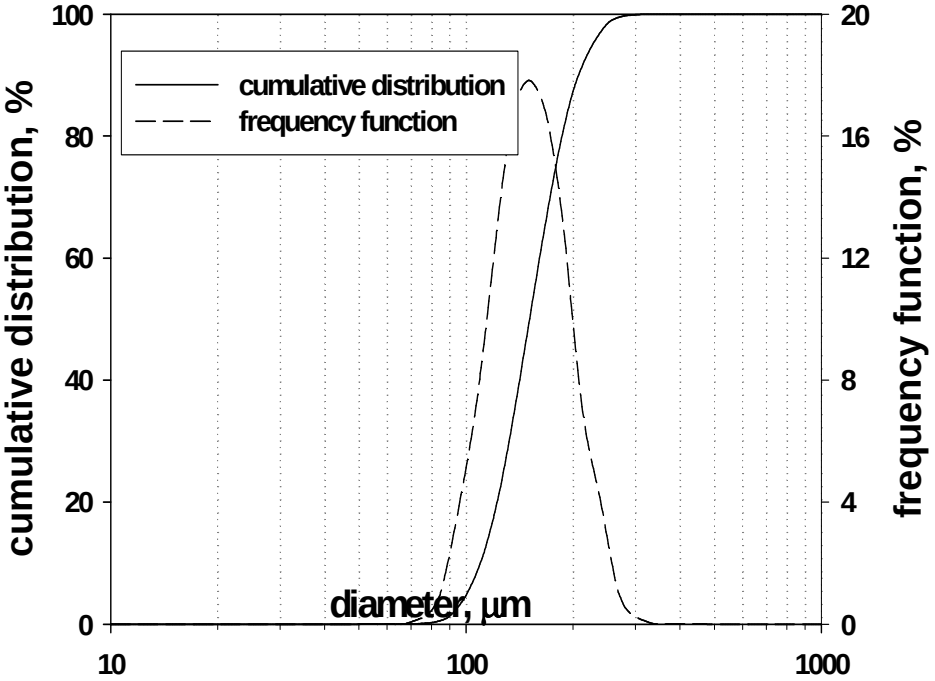

d_{Sauter}=146.5μm (Geldart A material)

Fluidization curves

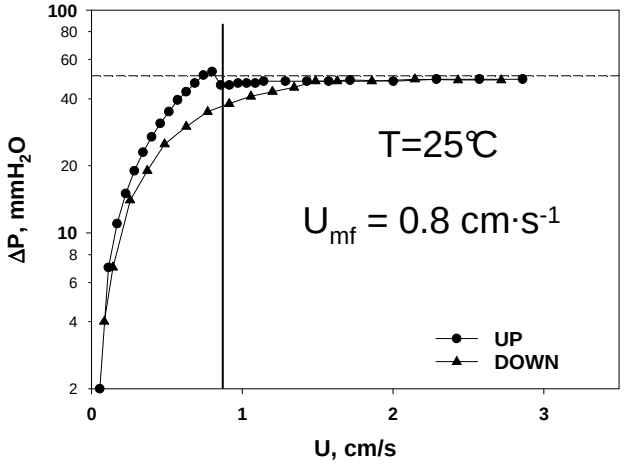

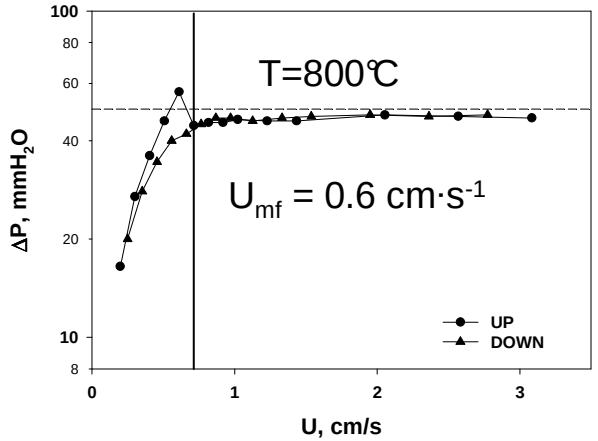

Characterization of attrition resistence of fillite

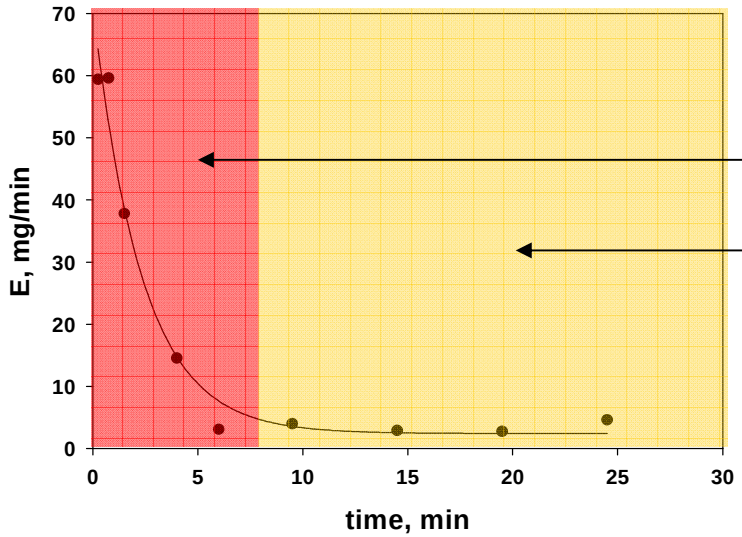

Attrition curve of cenospheres (125-212 microns), T=800℃, U=10 cm $\cdot s^{-1}$ (>10$\cdot U_{mf}$)

Zone a: peeling-off of particles asperities

Zone b: steady state mass loss of 2-3$\cdot 10^{-3}$g/min

According to a shrinking particle model **with no collapses** of the particle during its life-time inside the bed a relatively **short life-time** is expected.

Actually, particles collapsing is expected, which would lead to complete modification of fuidodynamic behaviour (elutriation or defluidization).

Critical aspect for **industrial applications** (costs linked to bed replacement)

Chemical looping combustion

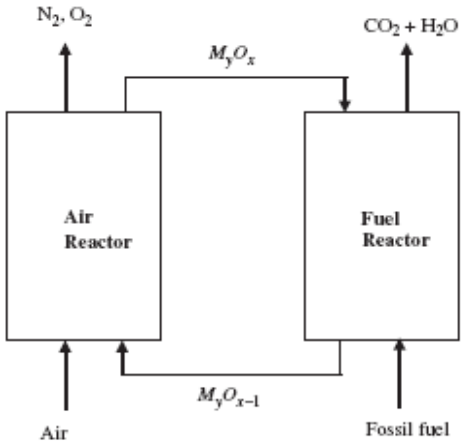

Johansson et al. 2006

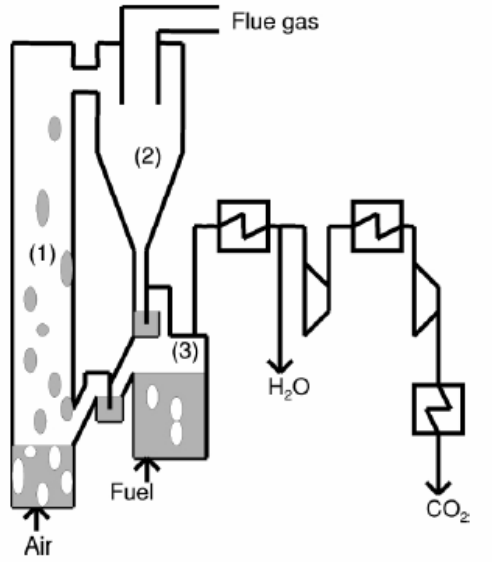

Johansson et al. 2006

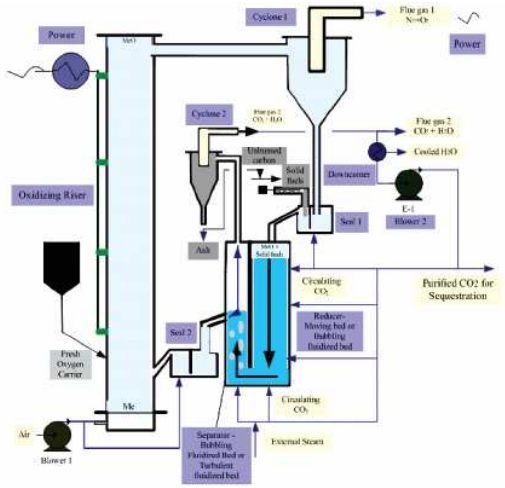

Yan Cao and Wei-Ping Pan 2006

Fuel reactor: $(2n + m)M_yO_x + C_nH_{2m} \rightarrow (2n + m)M_yO_{x-1} + mH_2O + nCO_2$

Air reactor: $(2n + m)M_yO_{x-1} + (n + \frac{1}{2}m)O_2 \rightarrow (2n + m)M_yO_x$

Net reaction: $C_nH_{2m} + (n + \frac{1}{2}m)O_2 \rightarrow mH_2O + nCO_2$

Oxygen carrier required properties

(i) Be stable under repeated oxidation/reduction cycles at high temperature.
(ii) Be fluidizable.
(iii) Be resistant to agglomeration.
(iv) Be mechanical resistant to the friction stress associated with high circulation of particles.
(v) Be environmentally benign and
(vi) Be economically feasible.

Main drawbacks of process

Strong chemical and thermal stresses of bed material in every cycle. Performance poor after low number of cycles in use.

Bed agglomeration

Developing of oxygen carrier for chemical looping combustion

No.	reduction reaction	melting point of the reduced metal form, °C	melting point of the oxidized metal form, °C	specific density of the reduced metal form ρ_R, kg/m³	specific density of the oxidized metal form ρ_O, kg/m³	moles of metal per mole of oxygen transfer (N), mol/mol	$(N x \rho_R)M/(N x \rho_R)Cu$ in reducer	$(N x \rho_O^{0.5})M/(N x \rho_O^{0.5})CuO$ in oxidizer
1	$2CuO + C = 2Cu + CO_2$	*1083*	*1026*	8920	6450	1	1.0	1.0
2	$2Cu_2O + C = 4Cu + CO_2$	*1083*	1235	8920	6000	*2*	*2.0*	*1.9*
3	$2NiO + C = 2Ni + CO_2$	1452	1452	8900	7450	1	1.0	1.1
4	$2Co_3O_4 + C = 6CoO + CO_2$	1480	**895**	8900	6070	**3**	**3.0**	**2.9**
5	$^1/_2Co_3O_4 + C = {}^3/_2Co + CO_2$	1480	**895**	8900	6070	0.75	0.7	0.7
6	$2CoO + C = 2Co + CO_2$	1480	1800	8900	5680	1	1.0	0.9
7	$6Mn_2O_3 + C = 4Mn_3O_4 + CO_2$	1564	*1080*	4856	4810	**6**	**3.3**	**5.2**
8	$2Mn_2O_3 + C = 4MnO + CO_2$	1650	*1080*	5180	4810	*2*	*1.2*	*1.7*
9	$^2/_3Mn_2O_3 + C = {}^4/_3Mn + CO_2$	1260	*1080*	7200	4810	0.67	0.5	0.6
10	$2Mn_3O_4 + C = 6MnO + CO_2$	1650	1564	5180	4856	**3**	**1.7**	**2.6**
11	$^1/_2Mn_3O_4 + C = {}^3/_2Mn + CO_2$	1260	1564	7200	4856	0.75	0.6	0.7
12	$2MnO + C = 2Mn + CO_2$	1260	1650	7200	5180	1	0.8	0.9
13	$6Fe_2O_3 + C = 4Fe_3O_4 + CO_2$	1538	1560	5200	5120	**6**	**3.5**	**5.3**
14	$2Fe_2O_3 + C = 4FeO + CO_2$	1420	1560	5700	5120	*2*	*1.3*	*1.8*
15	$^2/_3Fe_2O_3 + C = {}^4/_3Fe + CO_2$	1275	1560	7030	5120	0.67	0.5	0.6
16	$2Fe_3O_4 + C = 6FeO + CO_2$	1420	1538	5700	5200	**3**	**1.9**	**2.7**
17	$^1/_2Fe_3O_4 + C = {}^3/_2Fe + CO_2$	1275	1538	7030	5200	0.75	0.6	0.7
18	$2FeO + C = 2Fe + CO_2$	1275	1420	7030	5700	1	0.8	0.9
19	$2PbO + C = 2Pb + CO_2$	**327.5**	**886**	11340	8000	1	1.3	1.1
20	$2CdO + C = 2Cd + CO_2$	**320.9**	**900**	8650	8150	1	1.0	1.1

Yan Cao and Wei-Ping Pan 2006

Agglomeration phenomena or changing in the fluidization properties can occur due to the modification of catalyst in the reduction-oxidation step

Adding of a binder

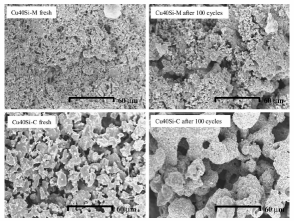

Prepared by mechanical mixing

Crushing strength (N/mm) of the extrudates prepared by different methods and using different binders

Preparation method	CuO (wt%)	Binder				
		Al_2O_3	Sepiolite	SiO_2	TiO_2	ZrO_2
M	80	3	4	22	66	6
M	60	0	0	20	59	2
M	40	0	0	17	43	1
C	40	–	–	14	–	–
I	20	–	–	27	–	–
I	30	–	–	–	60	–

L.F. de Diego et al. / Fuel 83 (2004) 1749–1757

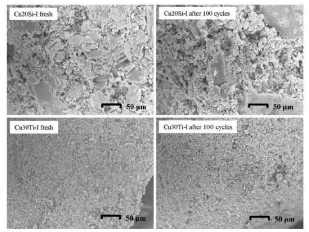

Prepared by impregnation

Attrition as suitable method for catalyst regeneration: catalytic methane decomposition process (TCD)

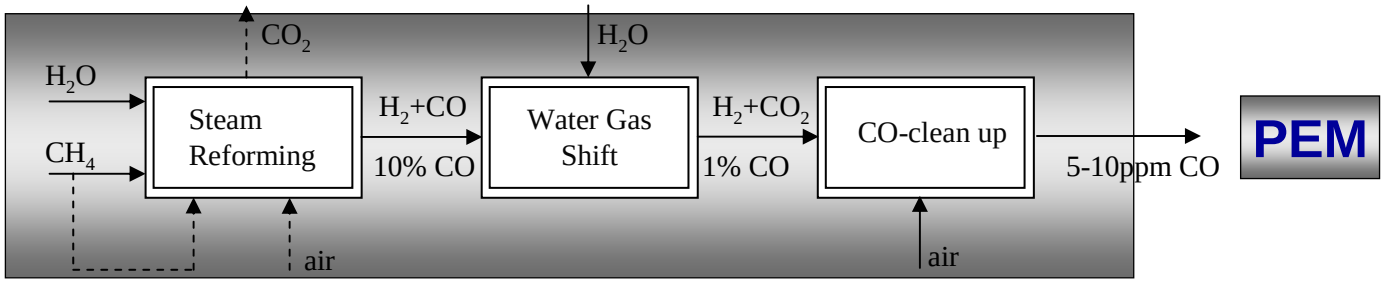

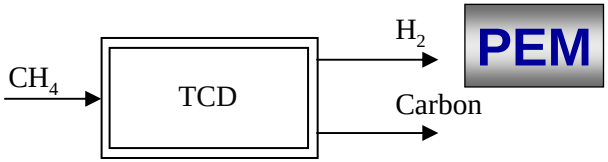

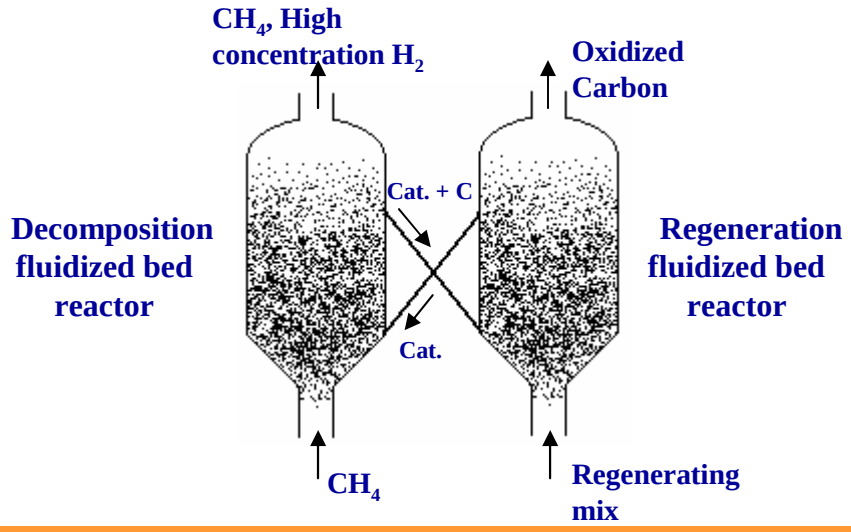

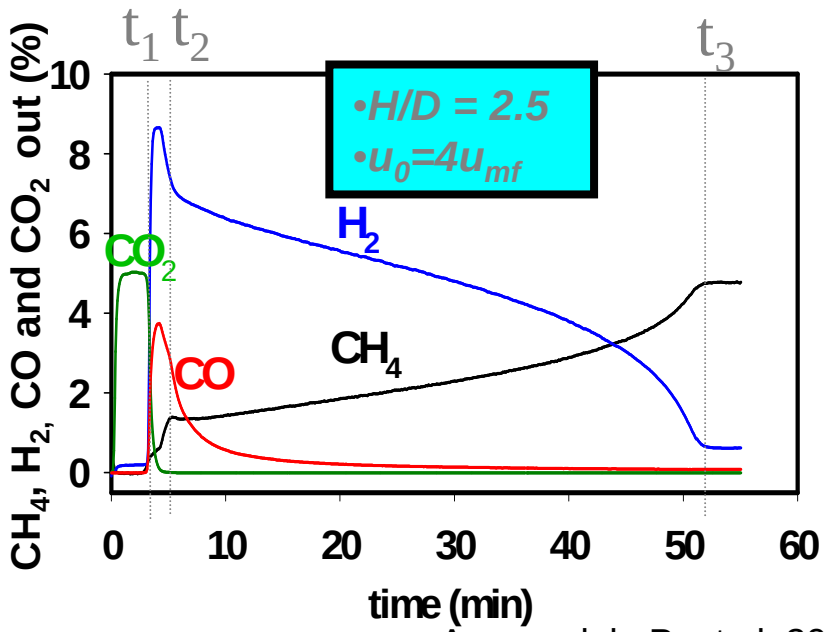

Ammendola P. et al. 2008

Regeneration of external surface of catalyst by attrition

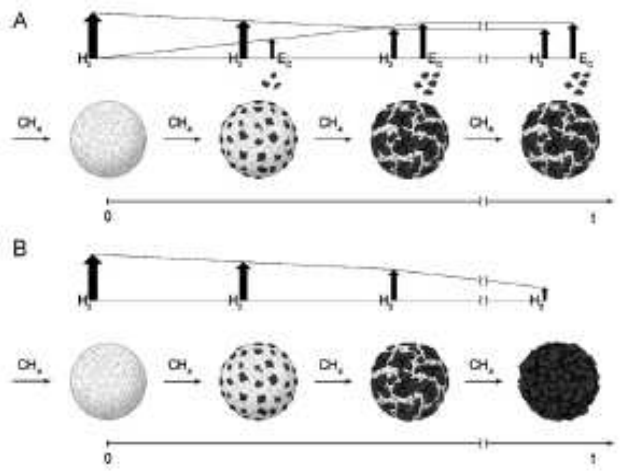

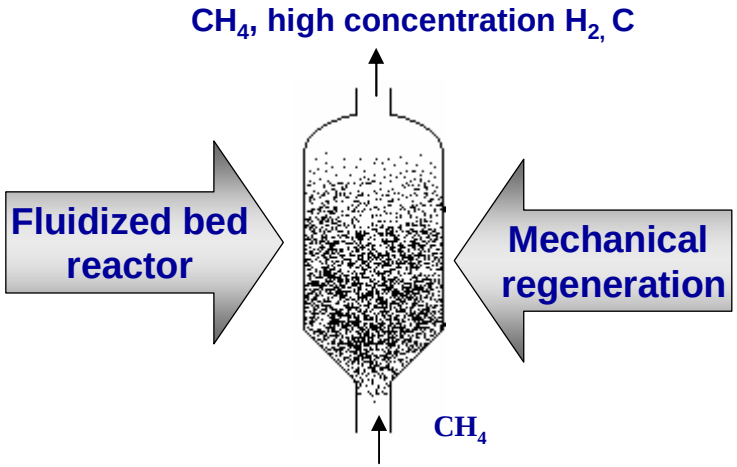

Total amount of carbon produced = **carbon deposed on the catalyst surface** + **Carbon collected in the elutriated**

Average attrition rate under reaction conditions: $2.7*10^{-5}$ g/min

Elutriated material elementary analysis: 10%wt C

Average attrition rate of deposited carbon: $2.7*10^{-6}$ g/min

Ammendola P. et al. 2008

Efficiency of attrition regeneration

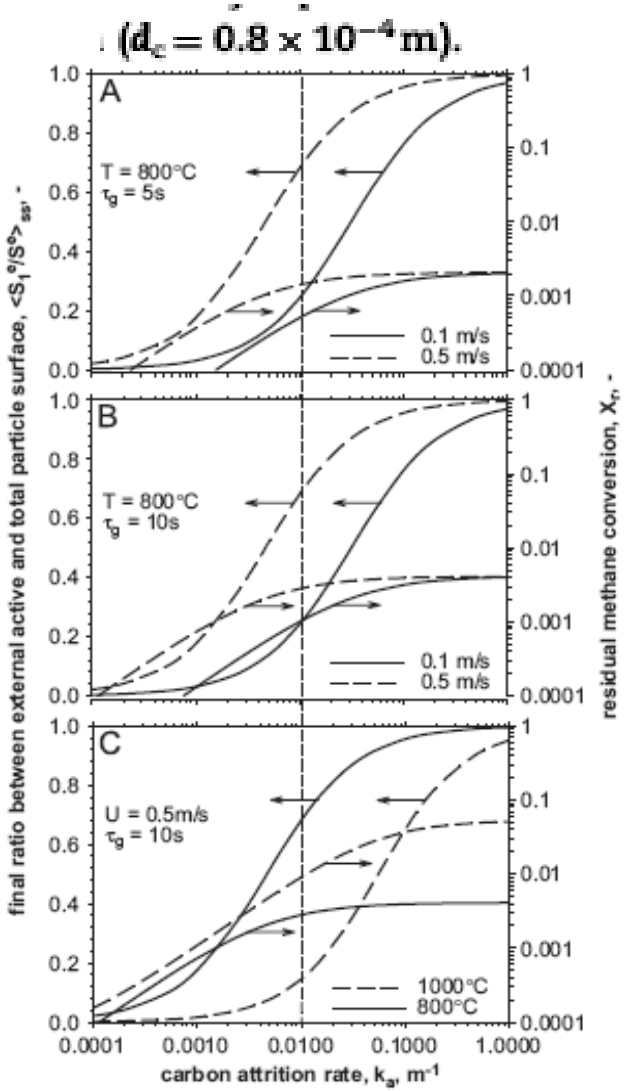

Use of a model to individuate the operative conditions In which attrition phenomena are relevant

This phenomenon can also affect the residual methane conversion when the contribution of the external surface of the particle to the reaction rate is high enough. This condition is emphasized by a high intrinsic kinetic rate and by a small size of catalyst particles

Ammendola P. et al. 2008

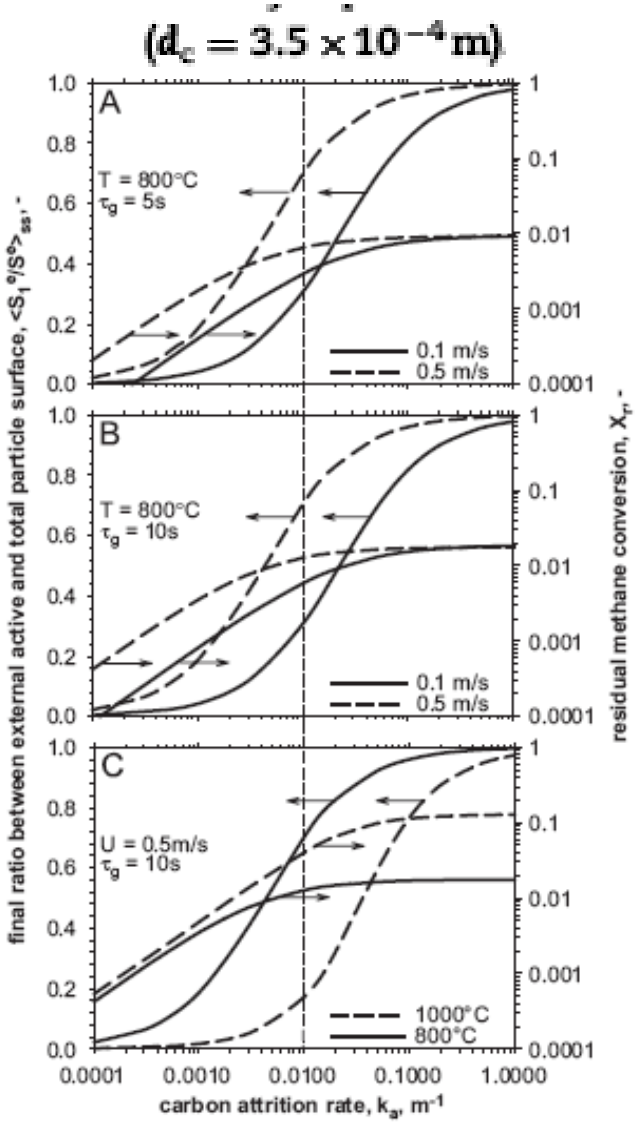

References

1. Ammendola P. Chirone R., Ruoppolo G., Russo G., Solimene R., Internationa Journal of Hydrogen Energy 33 (2008) 2679-2694
2. De Diego Luis F., Francisco Garcia-Labiano, Juan Adanez, Pilar Gayan, Alberto Abad, Beatriz M. Corbella, Josè Maria Palacios Fuel 83 (2004) 1749-1757
3. Johansson Marcus, Tobias Mattisson and Ander Lyngfelt Thermal Science: Vol. 10 (2006), No.3 pp.93-107
4. Geldart "Gas Fluidizat. Techn.", 1986 J. Wiley & Son
5. Iamarino M., Ammendola P., Chirone R., Pirone R., Ruoppolo G., Russo G. Industrial and Engineering Chemistry Research 45 (2006) 1009-1013
6. Iamarino M., Chirone R., Lisi L., Pirone R., Salatino P., Russo G. Catalysis today 75 (2002) 317-324
7. Ismagilov Z.R, R. A. Shkrabina, N.A. Koryabkina, Catalysis today 47 (1999) 51-71
8. Kunii D. and Levenspield O. Fludization Engineering 2°Ed. Butterworth-heinemann Boston, 1991
9. Perego C. and Villa P. L. Catalysis Today 34 (1997) 281-305
10. Yan Cao and Wei-Ping Pan Energy & Fuel 20 (2006) 1836-1844
11. Wen, C.Y. And Y.H. Yu, Aiche Journal, 12 (1966) 610